The Caribbean-North America-Cocos Triple Junction and the dynamics of the Polochic-Motagua fault systems: Pull-up and zipper models

Christine Authemayou, Gilles Brocard, C. Teyssier, T. Simon-Labric, A. Guttierrez, E. N. Chiquin, S. Moran

The Caribbean–North America–Cocos Triple Junction and the dynamics of the Polochic–Motagua fault systems: Pull-up and zipper models

C. Authemayou,[1,2] G. Brocard,[1,3] C. Teyssier,[1,4] T. Simon-Labric,[1,5] A. Guttiérrez,[6] E. N. Chiquín,[6] and S. Morán[6]

Received 13 October 2010; revised 4 March 2011; accepted 28 March 2011; published 25 June 2011.

[1] The Polochic-Motagua fault systems (PMFS) are part of the sinistral transform boundary between the North American and Caribbean plates. To the west, these systems interact with the subduction zone of the Cocos plate, forming a subduction-subduction-transform triple junction. The North American plate moves westward relative to the Caribbean plate. This movement does not affect the geometry of the subducted Cocos plate, which implies that deformation is accommodated entirely in the two overriding plates. Structural data, fault kinematic analysis, and geomorphic observations provide new elements that help to understand the late Cenozoic evolution of this triple junction. In the Miocene, extension and shortening occurred south and north of the Motagua fault, respectively. This strain regime migrated northward to the Polochic fault after the late Miocene. This shift is interpreted as a "pull-up" of North American blocks into the Caribbean realm. To the west, the PMFS interact with a trench-parallel fault zone that links the Tonala fault to the Jalpatagua fault. These faults bound a fore-arc sliver that is shared by the two overriding plates. We propose that the dextral Jalpatagua fault merges with the sinistral PMFS, leaving behind a suturing structure, the Tonala fault. This tectonic "zipper" allows the migration of the triple junction. As a result, the fore-arc sliver comes into contact with the North American plate and helps to maintain a linear subduction zone along the trailing edge of the Caribbean plate. All these processes currently make the triple junction increasingly diffuse as it propagates eastward and inland within both overriding plates.

Citation: Authemayou, C., G. Brocard, C. Teyssier, T. Simon-Labric, A. Guttiérrez, E. N. Chiquín, and S. Morán (2011), The Caribbean–North America–Cocos Triple Junction and the dynamics of the Polochic–Motagua fault systems: Pull-up and zipper models, *Tectonics*, *30*, TC3010, doi:10.1029/2010TC002814.

1. Introduction

[2] Guatemala is located within a plate interaction zone that involves the oceanic Cocos plate, the continental North American plate, and the Caribbean plate. The latter is an assembly of oceanic and continental fragments (Figure 1). This subduction-subduction-transform (SST) triple junction is referred to hereafter as the NACC triple junction. Off the Pacific coast, the Cocos plate is subducted beneath both the North American and Caribbean plates, which are separated by a sinistral transcurrent boundary. In Guatemala proper, the active boundary is comprised of two arcuate, subparallel fault systems, the Polochic and Motagua fault systems, which merge eastward; here, these coupled fault systems are referred to as the Polochic-Motagua Fault Systems or PMFS (Figures 1 and 2).

[3] The transform plate boundary has accommodated ~1100 km of strike-slip motion over the Cenozoic [*Rosencrantz et al.*, 1988]. A simple SST triple junction model predicts that the transform boundary should offset the Cocos subduction zone, generating a new Cocos–North America transform boundary that would lengthen over time (model A, Figure 3). This is not happening, and therefore the PMFS define a broad tectonic region that allows the migration and diffusion of the NACC junction (Figures 1 and 2). To the south of the PMFS, the deformation zone includes a series of N-S oriented grabens and the trench-

[1]Institute of Geology and Paleontology, Université of Lausanne, Lausanne, Switzerland.
[2]Now at Laboratoire Domaines Océaniques, UMR 6538, Université Européenne de Bretagne, Université de Brest, CNRS, IUEM, Plouzané, France.
[3]Now at Department of Earth and Environmental Sciences, University of Pennsylvania, Philadelphia, Pennsylvania, USA.
[4]Now at Department of Geology and Geophysics, University of Minnesota–Twin Cities, Minneapolis, Minnesota, USA.
[5]Now at ISterre, Université de Grenoble, Grenoble, France.
[6]Department of Geology, Universitad de San Carlos, Centro Universitario del Noreste, Cobán, Guatemala.

0278-7407/11/2010TC002814

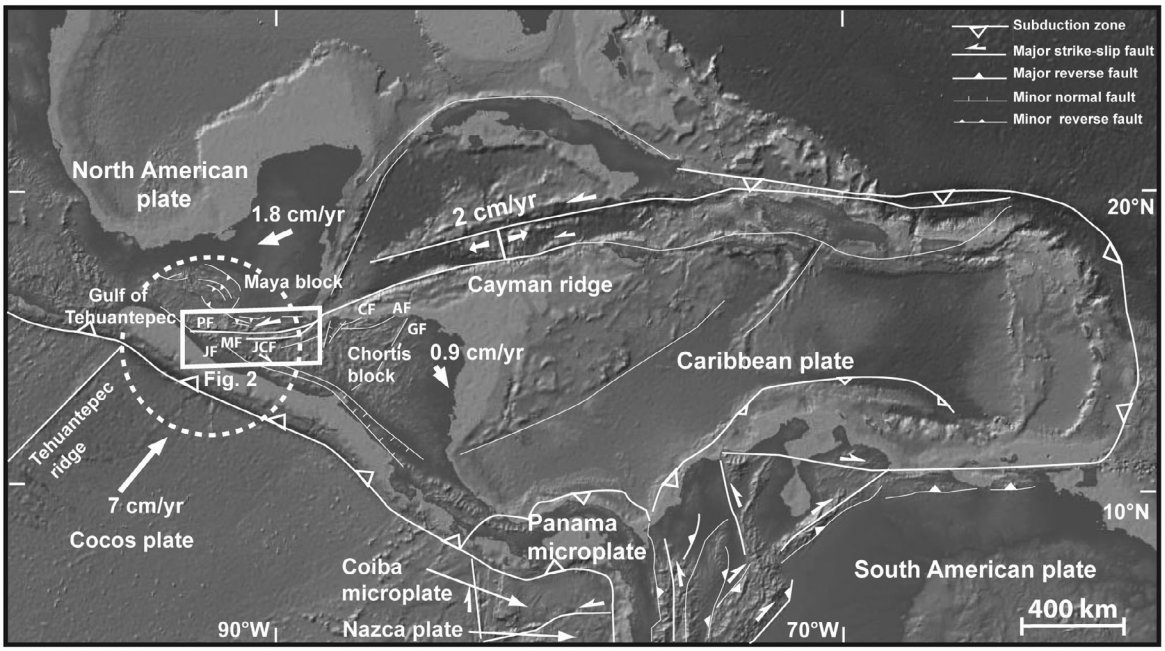

Figure 1. Geodynamics setting of Central America. White arrows indicate absolute plate motion [*Minster and Jordan*, 1978; *DeMets et al.*, 2000; *Morgan and Phipps Morgan*, 2007]. Dashed circle locates the region affected by the NACC triple junction. AF, Aguán fault; CF, Ceiba fault; GF, Guayape fault; JF, Jalpatagua fault; JCF, Jocotán-Chamalecón faults; MF, Motagua fault; PF, Polochic fault (see *Rogers and Mann* [2007, and reference therein] for the fault names).

parallel dextral Jalpatagua fault that tracks the volcanic arc [*Plafker*, 1976; *Burkart and Self*, 1985; *Lyon-Caen et al.*, 2006; *Rogers and Mann*, 2007]. North of the PMFS, the deformation zone comprises a series of NW-SE trending left-lateral strike-slip faults within the Chiapas belt, and the trench-parallel Tonala fault, which connects to the eastern end of the Polochic fault. The Tonala fault runs along the subduction zone at the same distance to the Cocos subduction zone as does the Jalpatagua fault (Figure 2) [*Guzmán-Spéziale and Meneses-Rocha*, 2000; *Andreani et al.*, 2008; C. Witt et al., The transpressive left-lateral Chiapas mountain chain and its buried front in the Tabasco plain, submitted to *Journal of the Geological Society*, 2011].

[4] This paper presents new structural and geomorphic data that document the integration, since the late Cenozoic, of the PMFS and neighboring faults into the tectonic system that now prevails at the NACC triple junction. We use previously mapped Mesozoic geological markers and newly mapped Neogene markers to document spatial and temporal changes in the dynamics of the PMFS. Stratigraphic boundaries are used to estimate the finite state of deformation. Tilting and offset of geomorphic markers of different ages (paleosurface, paleovalleys) are used to track recent deformation and to quantify rock uplift rates. These measurements are complemented by a regional fault kinematic analysis.

[5] We focus our study on the Neogene because the PMFS have been increasingly influenced by the approaching NACC triple junction during this period. We identify late Cenozoic structures and reconstruct their evolution during this key period. We evaluate whether this reconstruction is consistent with the predictions of several existing models and propose to recast some of the existing models and new observations into a new model, referred to as the "zipper" model (Figure 3).

2. Alternative Models for NACC Triple Junction

[6] Several models of NACC triple junction have been proposed to account for geological and geophysical observations. A first model considers that the transform boundary motion is totally absorbed by E-W extension south of the PMFS, within the Caribbean plate, associated with dextral strike-slip motion along the volcanic arc. This allows the Chortís block to escape eastward (model B, Figure 3) [*Plafker*, 1976; *Gordon and Muehlberger*, 1994; *Guzmán-Speziale*, 2001; *Rogers et al.*, 2002; *Lyon-Caen et al.*, 2006]. Another model suggests that extension in the Caribbean plate is not sufficient to absorb all the transform motion, and that a part of the transform motion is transferred to strike-slip and reverse faults in southern Mexico [*Guzmán-Speziale and Meneses-Rocha*, 2000]. *Andreani et al.* [2008] follow this model and delineate southern Mexico as a crustal block moving to the southeast with respect to North America. The displacement of this block generates extension through the central Trans-Mexican Volcanic Belt and strike-slip faulting in the Chiapas belt (model C, Figure 3). *Phipps Morgan et al.* [2008] consider that the Cocos plate is mechanically strong and does not tear in the triple junction, resulting in the formation of a continuous fore-arc sliver across the triple junction. Intraplate deformation is taking place behind this sliver in the form of shortening and extension, north and south of the transform boundary, respectively (model D, Figure 3).

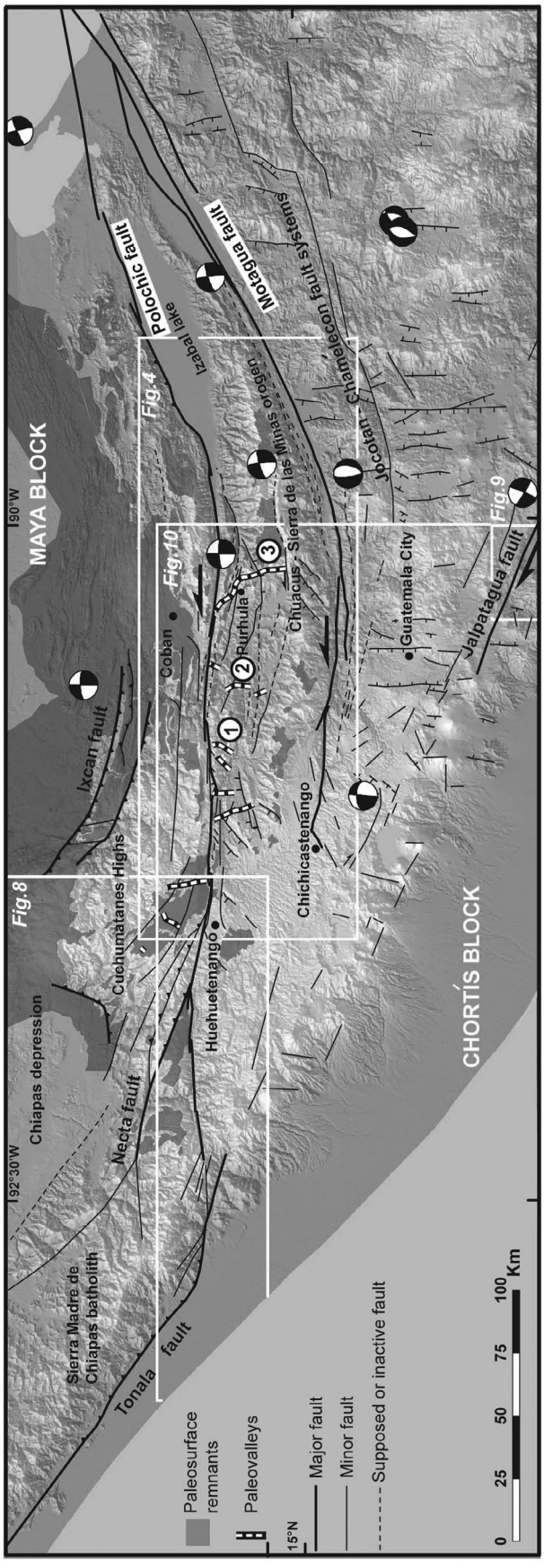

Figure 2. Traces of fault associated with the North American–Caribbean transform plate boundary in Guatemala. Focal mechanisms according to a maximum depth are from the centroid moment tensor catalog. Location of geomorphologic markers discovered by *Brocard et al.* [2011b] is displayed with gray surfaces for the middle Miocene Paleosurface remnants and with dashed white lines on black ground color for the paleovalleys. The paleosurface is only distinguished north of the Motagua fault. Circled 1, 2, and 3 indicate the paleovalleys used in the text for analyzing their deformation. Location is given on Figure 1.

[7] The change of angle between the plate motion vector and the azimuth of the arcuate plate margin fault was discussed to explain extension eastward and shortening westward close to the transform zone (model E, Figure 3) [*Burkart and Self*, 1985; *DeMets et al.*, 2000; *Rogers and Mann*, 2007]. Numerical modeling, based on seismic tensors and GPS velocity fields [*Álvarez-Gómez et al.*, 2008; *Rodriguez et al.*, 2009], assigns an important role to the fore-arc sliver and the arcuate shape of the transform boundary. In this model the western edge of the Chortís block is regarded as partially pinned to North America, and weak coupling occurs in the fore-arc sliver across the Caribbean/Cocos subduction interface, while stronger coupling occurs across the North American/Cocos subduction interface [*Franco et al.*, 2009]. The seismotectonic model of *Guzmán-Speziale* [2009] arrives at the same conclusion, inasmuch as the Chortís block is being extruded toward the ESE by convergence between the North America and Cocos plates.

[8] The model advocated here (model F, Figure 3) is one in which the fore-arc tectonic sliver plays a major role in the dynamics of the triple junction. The eastward retreat of the Caribbean plate relative to the trench and the differential coupling along the subduction interface across the triple junction force the fore-arc sliver to occupy the space left by the departing trailing edge of the Caribbean plate. As a result, the fore-arc sliver comes to lean against the North American plate (model F, Figure 3). The sinistral transform boundary, on one side, and the dextral strike-slip fault bounding the sliver on the other side, come side to side, suture, and leave the northern part of the fore-arc sliver stranded along North America. The locus of suturing migrates progressively southeastward along the conjugate faults, much like a "zipper." As a result, the triple junction migrates eastward with the bulk of the Caribbean plate.

3. Regional Tectonic Patterns

3.1. The Transform North American/Caribbean Plate Boundary

[9] The North American plate is separated from the Caribbean plate by a left-lateral transform boundary that accommodates the westward migration of the North American plate (Figure 1). In Guatemala the transform boundary brings into contact two continental blocks, the North American Maya block and the Caribbean Chortís block. The arcuate, 500 km long transform boundary is composed of two roughly E-W trending, active fault systems located a maximum of 50 km apart (the PMFS): the Motagua fault to

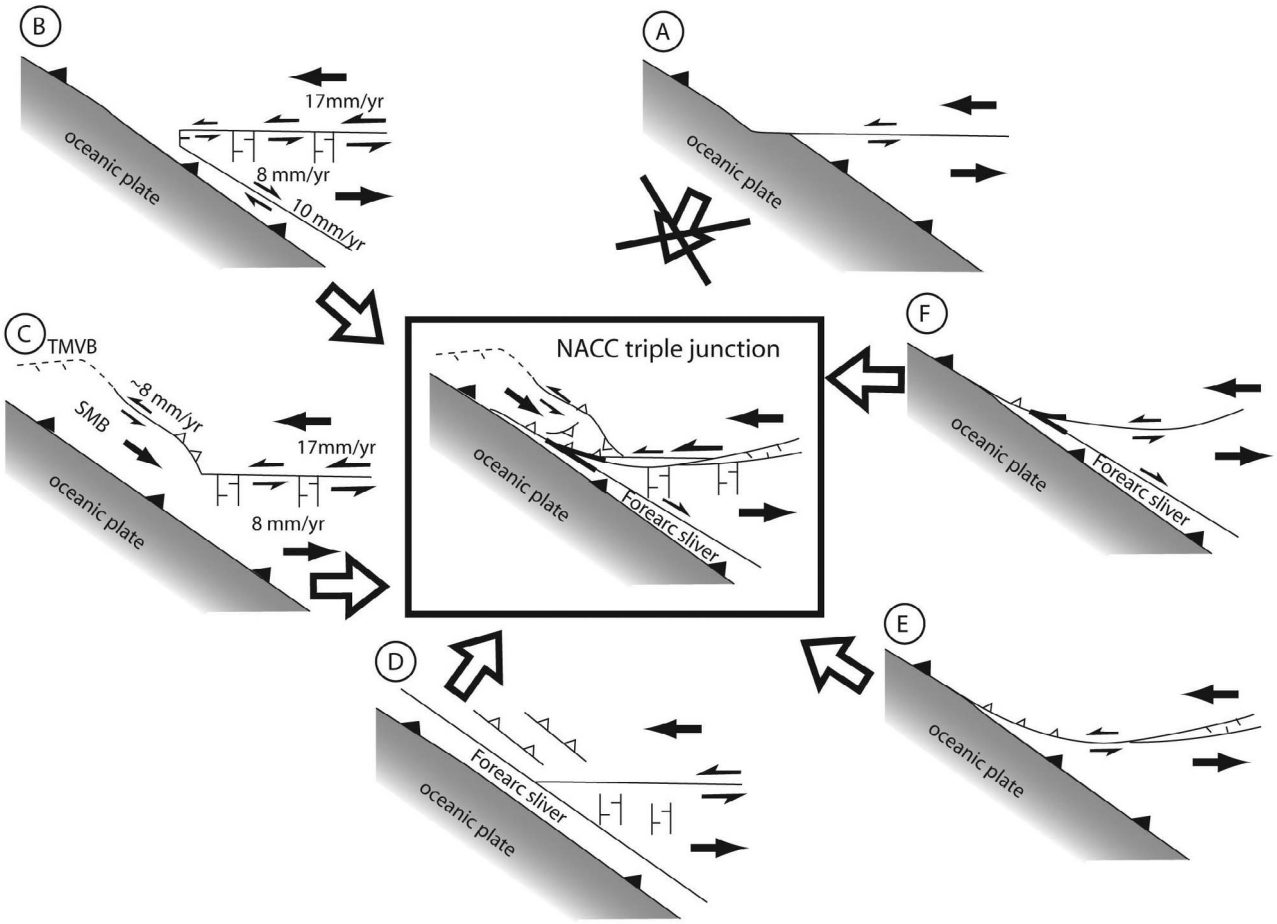

Figure 3. Different kinematics models of triple plate junction that explains the NACC triple junction migration. Model A corresponds to the geometry for a stable triple plate junction if the oceanic plate should tear at the triple junction. Model B comes from *Plafker* [1976]; *Gordon and Muehlberger* [1994], *Guzmán-Speziale* [2001], *Rogers et al.* [2002], and *Lyon-Caen et al.* [2006]. Model C is suggested by *Guzmán-Speziale and Meneses-Rocha* [2000] and *Andreani et al.* [2008]. SMB, Southern Mexico block, TMVB, Trans-Mexican volcanic belt. Model D was proposed by *Phipps Morgan et al.* [2008]. Model E is discussed by *Burkart and Self* [1985], *DeMets et al.* [2000], *Rogers and Mann* [2007], and *Rodriguez et al.* [2009]. Model F illustrates the "zipper" process discussed in this paper. Thick black portions of the dextral and sinistral faults show the merging of these faults.

the south and the Polochic fault to the north (Figures 1 and 2) [*Franco et al.*, 2009; *Suski et al.*, 2010]. The transform system also includes a series of large shears distributed across the Chortís block: the Jocotán-Chamelecón faults, the Ceiba fault, the Aguán fault and the Guayape fault (Figure 1) [*Burkart and Self*, 1985; *Burkart*, 1994; *Gordon and Muehlberger*, 1994; *Rogers and Mann*, 2007; *Silva-Romo*, 2008].

[10] To the east, the PMFS connects to transform faults that bound the Cayman oceanic spreading center [*Pindell et al.*, 2005]. To the west, the Polochic fault connects to the Tonala fault [*Carfantan*, 1976], a transcurrent plate boundary fault that has permitted the transfer of the Chortís block from Mexico to the Caribbean plate during the Cenozoic [*Pindell et al.*, 2005; *Ratschbacher et al.*, 2009]. Geochronological and thermochronological studies of mylonites from the Tonala and Polochic shear zones, and from plutons that intruded these faults, suggest simultaneous fault activity between ~15 Ma and ~5 Ma [*Wawrzyniec et al.*, 2005; *Ratschbacher et al.*, 2009].

[11] Finite offsets of the 40 Ma old and 15 Ma old magmatic belts in southern Mexico and in the Chortís block, suggest that 700 km of displacement was accommodated along the PMFS prior to c. Fifteen Ma. Since that time, 300 km displacement took place along the Motagua fault and over 100 km on the Polochic fault [*Ratschbacher et al.*, 2009]. These estimates agree well with the total motion of 130 km along the Polochic fault [*Burkart*, 1983] and contradict the limited displacement argued by *Anderson et al.* [1985] for the Polochic fault during Cenozoic time. *Brocard et al.* [2011] showed that only 25 km out of these 130 km have occurred since 10–7 Ma, suggesting contemporaneous activity on the Motagua fault during this period, contrary to the interpretation of *Burkart* [1994].

3.2. Anatomy of the Current NACC Triple Junction

[12] The PMFS represent one arm of the triple junction between the Cocos, North American, and Caribbean plates. Some authors suggested that the PMFS join the Middle American trench in the Gulf of Tehuantepec [*Anderson and Schmidt*, 1983; *Pindell et al.*, 1988; *White and Harlow*, 1993; *Schaaf et al.*, 1995], while others suggested that these boundaries intersect directly west of the PMFS [*Keppie and Morán-Zenteno*, 2005; *James*, 2006]. The latter view is not supported; there is no clear intersection between the projected trace of the PMFS and the linear subduction zone [*Muehlberger and Ritchie*, 1975; *Carfantan*, 1976]. The traces of the Motagua fault and Jocotán-Chamelecón faults disappear in western Guatemala within late Cenozoic to Quaternary volcanic deposits. The Polochic fault, on the other hand, straddles the entire continental domain but does not seem to enter the Pacific Ocean to reach the Middle American trench (Figure 2). The location of the NACC triple junction is actually more diffuse. It integrates the northwestern part of Guatemala, southern Mexico, and a large part of the Chortís block [*Plafker*, 1976; *Burkart*, 1983; *Gordon and Muehlberger*, 1994; *Guzmán-Speziale and Meneses-Rocha*, 2000; *Guzmán-Speziale*, 2001; *Lyon-Caen et al.*, 2006; *Andreani et al.*, 2008; *Phipps Morgan et al.*, 2008; *Rodriguez et al.*, 2009].

[13] North of the PMFS, in southern Mexico, two shortening domains affect the Maya block (Figure 1). An E-W trending, 80 km wide fold-and-thrust belt runs alongside the PMFS and has been associated with Paleocene-Eocene Laramide orogenic events [*Donnelly et al.*, 1990]. To the NW, this range is relayed by the arcuate post-middle Miocene Chiapas fold-and-thrust belt. The Chiapas belt is crosscut by an array of west to NW trending left-lateral strike-slip faults that may have developed in close association with the PMFS [*Guzmán-Speziale and Meneses-Rocha*, 2000; *Andreani et al.*, 2008; *Guzmán-Speziale*, 2010]. Along the Pacific coast of Mexico, the Chiapas belt is bordered by the Permo-Triassic Sierra Madre de Chiapas batholiths. The Sierra Madre de Chiapas is in turn bounded to the west by the Tonala fault [*Weber et al.*, 2005, and references therein] (Figure 2).

[14] South of the PMFS, a series of active N-S grabens affect the Chortís block and fragment the inactive Jocotán-Chamelecón fault system [*Plafker*, 1976; *Rogers et al.*, 2002] (Figure 2). Some of these grabens are connected to the Motagua fault [*Plafker*, 1976] and developed concurrently with the epeirogenic uplift that has affected the Chortís block. This uplift has been ascribed to slab break off underneath Central America and related to a late Miocene thermal event [*Rogers et al.*, 2002] that imprinted 11.3–7.9 Ma apatite fission track ages to basements rocks in a graben flank [*Ratschbacher et al.*, 2009]. To the SW, the Jalpatagua dextral fault runs parallel to the Pacific coast and closely tracks the active volcanic arc (Figures 1 and 2). The fault isolates a fore-arc sliver from the bulk of the Caribbean plate [*DeMets*, 2001], and Quaternary volcanic deposits are affected by right-lateral strike-slip displacement [*Wunderman and Rose*, 1984; *Duffield et al.*, 1992]. Such movement is also observed along structures that are located in the continuation of the Jalpatagua fault in Costa Rica, Nicaragua, and El Salvador [*La Femina et al.*, 2002]. The WNW trending dextral Jalpatagua fault and the E-W trending sinistral PMFS enclose a large wedge-shaped domain in the Chortís block, which tapers to the west, near Chichicastenango in Guatemala (Figure 2).

4. New Geomorphic and Structural Analyses

4.1. Deformation Between the Polochic and Motagua Faults

4.1.1. Geologic Structure

[15] Ongoing deformation within the PMFS activates a tectonic pattern inherited from former transpressional events that have affected the plate boundary since Late Cretaceous time [*Kesler*, 1970; *Donnelly et al.*, 1990; *Ortega-Gutiérrez et al.*, 2004]. Three range-parallel rock belts with distinct deformational and metamorphic histories are usually distinguished between the Polochic and Motagua faults (Figure 4). The Polochic fault disrupts the northernmost belt, a fold-and-thrust belt that involves a sedimentary cover composed of Mississippian to Permian siliciclastic rocks, shale, and limestone, Jurassic red beds, and Cretaceous limestone [*Walper*, 1960; *McBirney*, 1963; *Burkart*, 1978] (Figure 4). The sedimentary cover has been overthrust by Mesozoic ophiolitic nappes (Figure 4 and cross section A, Figure 5); these nappes are remnants of a Caribbean oceanic domain that was obducted northward onto the Maya block during Late Cretaceous [*Beccaluva et al.*, 1995; *Harlow et al.*, 2004; *Brueckner et al.*, 2009]. The ophiolitic nappes and the underlying sedimentary cover were deformed together in open folds during the Paleocene-Eocene Lamaride orogeny [*Dengo*, 1982; *Burkart*, 1983; *Donnelly et al.*, 1990]. From north to south, fold axes change in strike from W-E and SW-NE to WNW-ESE across the Polochic fault (Figure 4). WNW trending thrusts are associated with the WNW trending folds [*Dengo*, 1982; *Burkart*, 1983]. Some WNW trending folds are encountered north of the western part of the Polochic fault (Figure 4). They were correlated with the WNW trending folds south of the fault located more than 130 km away [*Burkart*, 1978; *Burkart et al.*, 1987]. Their correspondence has been used, in addition to the offset of river networks to infer a 132 ± 5 km sinistral displacement of the Polochic fault after the Paleocene-Eocene orogeny [*Dengo*, 1982; *Burkart*, 1983].

[16] The tectonic sliver bracketed by the Polochic and Motagua faults is hereafter referred to as the Polochic-Motagua sliver. Within this sliver, the Laramide fold-and-thrust belt is in turn overthrust by the Salamá Formation, a low-grade metamorphic domain (Figure 4 and cross section A, Figure 5), consisting of Cambrian-Permian sedimentary rocks intruded by granitic bodies [*McBirney*, 1963; *Ortega-Gutiérrez et al.*, 2004]. To the south, this low-grade metamorphic unit is in turn overthrust along the south dipping, high-angle Baja Verapaz shear zone by the higher-grade Chuacús complex [*McBirney*, 1963; *Ortega-Gutiérrez et al.*, 2007] (Figure 4 and cross section A, Figure 5). The contact shows top-to-the-NNE reverse shearing of Late Cretaceous age [*Ortega-Gutiérrez et al.*, 2007].

[17] The Chuacús complex is the southernmost belt and forms the core of the Chuacús-Sierra de las Minas range (Figure 2). Widespread ductile left-lateral wrenching imprinted a strong, orogen-parallel steep fabric to the Chuacús complex [*Kesler*, 1970; *Donnelly et al.*, 1990;

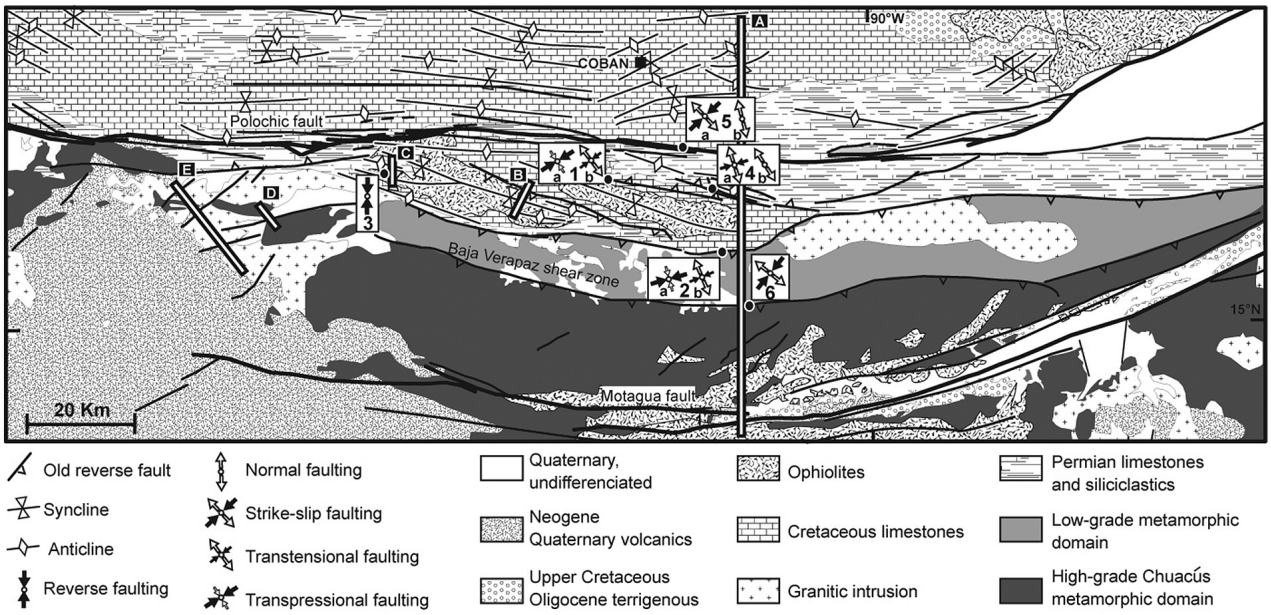

Figure 4. Geology of the PMFS (compiled after *Anderson et al.* [1985], *Burkart et al.* [1987], *Donnelly et al.* [1975], *Kesler et al.* [1970], *McBirney* [1963], and our proper observations). White bands associated with capital letter in a square indicate locations of geologic cross sections A, B, C, D, and E of Figure 5. Results are of fault slip data inversions. Stations refer to Figure 7; small letter indicate the relative chronology of fault slip data sets. Location is shown on Figure 2.

Gordon and Avé Lallemant, 1995; *Ortega-Gutiérrez et al.*, 2004]. The 20–30 km wide complex (Figure 4) consists of a core of alternating micaschists and gneisses fringed by more diverse assemblages of amphibolite, marble, and migmatite [*McBirney*, 1963]. Metamorphism reaches amphibolite grade, but inclusions of eclogitic rocks suggest that the Late Cretaceous event peaked in eclogitic conditions [*Ortega-Gutiérrez et al.*, 2004; *Harlow et al.*, 2004]. Along its southern border, next to the Motagua fault, the Chuacús complex is overthrust by ophiolitic mélanges containing Cretaceous high-pressure rocks [*Harlow et al.*, 2004] (Figure 4 and cross section A, Figure 5).

[18] The overall southward increase of metamorphic grade from the Polochic fault to the Motagua fault is consistent with the exhumation of deeper rocks along the suture zone. South of the Motagua fault, ophiolitic bodies of the Cretaceous El Tambor Formation were thrust onto the Las Ovejas high-grade metamorphic complex, which is in turn thrust onto the Chortís basement. El Tambor is older than the northern ophiolitic unit and likely of different origin [*McBirney*, 1963; *Donnelly et al.*, 1990; *Beccaluva et al.*, 1995; *Harlow et al.*, 2004; *Ortega-Gutiérrez et al.*, 2007].

[19] As a whole, we notice that the inner structure of the Polochic-Motagua sliver is that of a curved, E-W to NW trending narrow thrust system of imbricate and sigmoidal domains (Figure 4). This geometry gives the belt the characteristics of a left-lateral transpressional zone.

4.1.2. Neogene Geomorphic and Geologic Markers

[20] The Mayan paleosurface and the paleovalleys that are preserved in the region provide two types of Neogene markers to evaluate late Cenozoic deformation within the PMFS (Figure 2).

4.1.2.1. The Mayan Paleosurface

[21] The Mayan paleosurface is a widespread planation surface that has developed over much of the southern Maya block in the Miocene. It has been identified north of the Polochic fault and over the Polochic-Motagua sliver [*Brocard et al.*, 2011]. The Mayan paleosurface is extensively preserved on the highest summits of the range, perched at elevations of 2400–2500 m (Figure 2). In the lowlands, north of the Polochic fault, the paleosurface progressively disappears within the foreland plain. On crystalline siliceous rocks, it is underlain by a thick saprolite [*McBirney*, 1963], while on carbonates it has been extensively riddled by the development of a typical cockpit karst.

Figure 5. Geological cross sections through the Polochic-Motagua sliver. Geologic cross section A of PMFS crosses the Cahabón River paleovalley. Vertical tectonic offsets of the middle Miocene paleosurface and the mid-Quaternary paleovalley are indicated on top of the cross section. Geologic cross sections B and C traverse the Chicruz and Sicaché paleovalleys, respectively. Crosses are precise laser topographic measurements projected from the sides of the paleovalley onto the cross section axis. Dashed lines indicate the boundaries of old river deposits and felsic volcanic sheet. Cross section C is associated with Ar-Ar istopic data shown by step heating (S1, S2, S3). Cross sections D and E are located in the southwestern termination of the Polochic fault. Gray rectangles and gray outlined rectangles depict paleosurface and paleovalley remnants, respectively. Gray lines are interpolated surface of geomorphic marker remnants. Locations are shown on Figure 4.

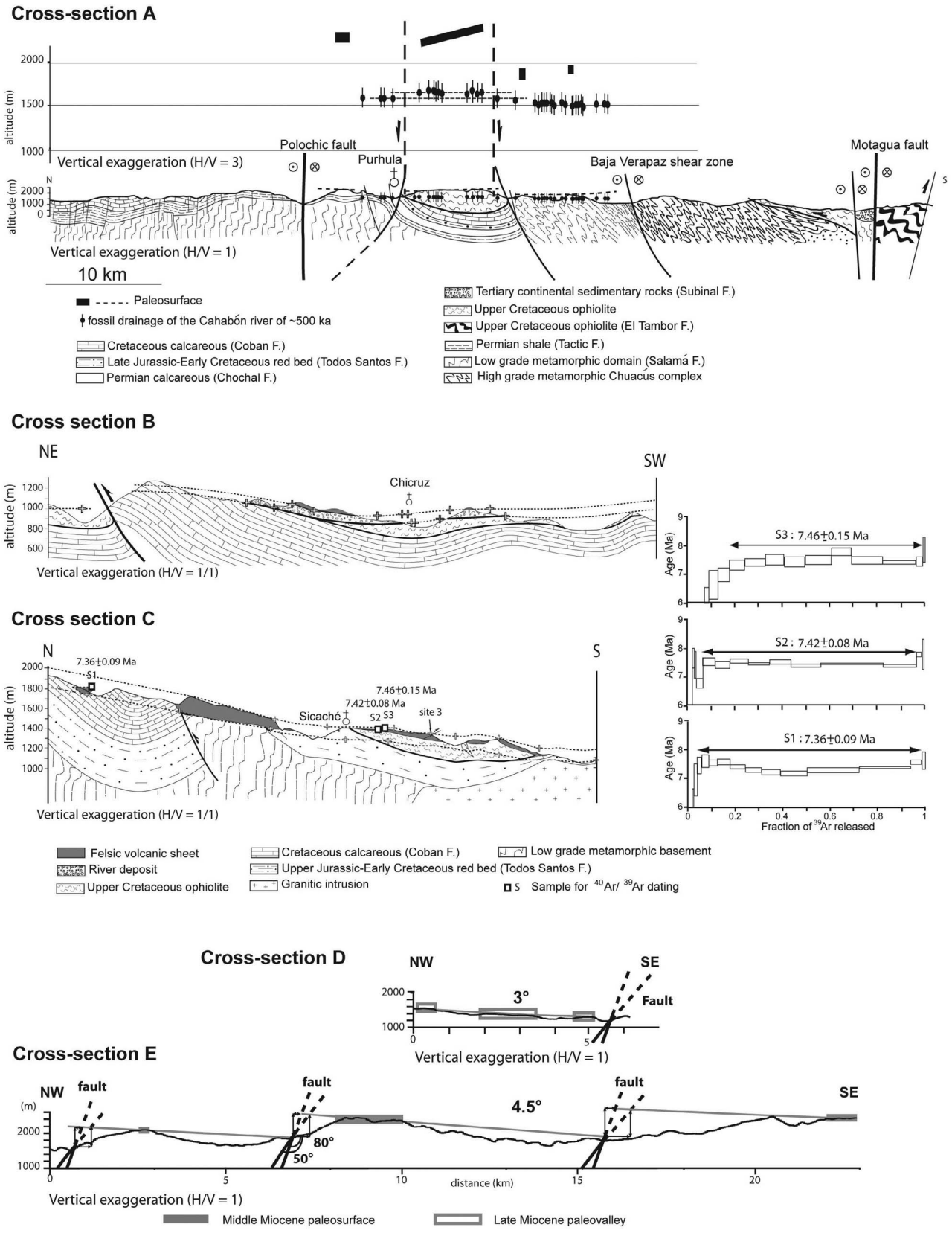
Cross-section A
altitude (m)
2000
1500
1000
Vertical exaggeration (H/V = 3)
Polochic fault
Purhula
Baja Verapaz shear zone
Motagua fault
N
S
altitude (m)
2000
1000
0
Vertical exaggeration (H/V = 1)
10 km
Paleosurface
fossil drainage of the Cahabón river of ~500 ka
Cretaceous calcareous (Coban F.)
Late Jurassic-Early Cretaceous red bed (Todos Santos F.)
Permian calcareous (Chochal F.)
Tertiary continental sedimentary rocks (Subinal F.)
Upper Cretaceous ophiolite
Upper Cretaceous ophiolite (El Tambor F.)
Permian shale (Tactic F.)
Low grade metamorphic domain (Salamá F.)
High grade metamorphic Chuacús complex
Cross section B
NE
SW
Chicruz
altitude (m)
1200
1000
800
600
Vertical exaggeration (H/V = 1/1)
S3 : 7.46±0.15 Ma
S2 : 7.42±0.08 Ma
S1 : 7.36±0.09 Ma
Age (Ma)
Fraction of 39Ar released
Cross section C
N
S
7.36±0.09 Ma
S1
7.46±0.15 Ma
7.42±0.08 Ma
Sicaché
S2 S3
site 3
altitude (m)
2000
1800
1600
1400
1200
1000
Vertical exaggeration (H/V = 1/1)
Felsic volcanic sheet
River deposit
Upper Cretaceous ophiolite
Cretaceous calcareous (Coban F.)
Upper Jurassic-Early Cretaceous red bed (Todos Santos F.)
Granitic intrusion
Low grade metamorphic basement
S Sample for 40Ar/ 39Ar dating
Cross-section D
NW
SE
3°
Fault
2000
1000
Vertical exaggeration (H/V = 1)
Cross-section E
NW
fault
fault
fault
SE
(m)
2000
1000
4.5°
80°
50°
distance (km)
Vertical exaggeration (H/V = 1)
Middle Miocene paleosurface
Late Miocene paleovalley

Figure 5

Such surfaces are, and have long been interpreted as the remnants of peneplains, etchplains or pediplains [*Widdowson*, 1997].

[22] The paleosurface could be synchronous with the ubiquitous peneplain that developed over the Chortís block as a low, rolling country, not far above sea level [*Williams and McBirney*, 1969]. This peneplain was buried below up to 1 km of ignimbrite sheets during an ignimbrite flare-up that peaked at 14–15 Ma [*Sigurdsson et al.*, 2000]. Ignimbrite sheets were deposited between 17 and 13 Ma, providing a minimum age for the paleosurface [*Jordan et al.*, 2007]. After burial, the surface was tectonically disrupted between 10.5 Ma and 4 Ma and uplifted 800–1000 m [*Dengo et al.*, 1970; *Rogers et al.*, 2002; *Jordan et al.*, 2007]. This surface is to be distinguished from that discussed by *Rogers et al.* [2002]; they consider the younger depositional surface on top of the ignimbrites whereas we used the peneplain surface beneath the volcanic deposits.

[23] North of the PMFS, Eocene folds are completely beveled by the paleosurface [*Anderson et al.*, 1973; *Walper*, 1960]. The paleosurface is thus younger than the Eocene folds, and older than 7 Ma old paleovalleys that are incised within it (see below). The paleosurface likely started to be dissected during the middle Miocene, like its southern equivalent on the Chortís block [*Williams and McBirney*, 1969].

4.1.2.2. Paleovalleys

[24] The second group of markers is a series of 12 paleovalleys that are incised within the Mayan paleosurface [*Brocard et al.*, 2011]. These paleovalleys straddle various geological formations, such as the crystalline basement, the ophiolite, and Mesozoic sandstone and limestone (Figures 4 and 5). The preserved segment of the paleovalley of Sicaché (cross section C, Figure 5) lies within 4–10 km of the Polochic fault whereas the preserved segment of the paleovalley of Chicruz, 30 km further east (cross section B, Figure 5), is located farther from the fault (12–17 km) (Figure 2). Junction angle of tributaries, gravel composition, and clast imbrication show that the valleys were carved by north flowing rivers. These valley remnants retain felsic volcaniclastic sheets (cross section C, Figure 5) that have yielded $^{40}Ar/^{39}Ar$ ages of 7.4 Ma in Sicaché [*Brocard et al.*, 2011]. Geochemical similarities among volcanic ashes in the paleovalleys of Sicaché and Chicruz suggest that they were produced by the same volcanic eruptions. The paleovalley of the Cahabón River, 50 km further east (cross section A, Figure 5) retains river sediments that we have dated by a combination of magnetic polarity measurements and ^{10}Be-^{26}Al burial dating of the sediments. They yield an abandonment ages of 0.5–1.0 Ma (G. Brocard et al., River network vulnerability to rearrangement during incipient faulting: Velocity and mechanisms along the Cahabón River, Guatemala, from combined ^{10}Be-^{26}Al, magnetic polarity and electrical resistivity tomography measurements, submitted to *American Journal of Science*, 2011).

4.1.3. Deformation of Neogene Markers

[25] The Mayan paleosurface was reconstructed in order to identify surface deformations over the PMFS. To identify and map the remnants of the Mayan paleosurface, we combined field observations with satellite image interpretation, and analysis with filter processing of the 3 arc second Shuttle Radar Topographic Mission (SRTM) digital elevation model (Figure 2). The eroded surface between preserved remnants was reconstructed using a cubic spleen interpolation. This technique is the best suited since surface deformation appears to be dominated by folding. The interpolation was reprocessed, however, to allow the surface to break freely across identified tectonic discontinuities (Figure 6). The resulting paleosurface elevation is regarded as accurate on average within ±100 m over the area of concern.

[26] The surface is mildly folded and disrupted, but strongly uplifted at a regional scale. The areas of highest uplift are located in the Cuchumatanes Highs (3800 m), north of the Polochic fault, and the Sierra de las Minas (3000 m), near the Motagua fault (Figure 6). Folding affects the paleosurface with a 5–10 km wavelength and reactivates preexisting folds of the Lamaride belt (Figure 6). This folding can be ascribed to a minor component of shortening resulting from a slight obliquity in strike between the Polochic fault and the interplate motion vector, as it has been proposed by *Rodriguez et al.* [2009] in the case of the Motagua fault. North of the Polochic fault, most of these postpaleosurface folds are parallel to the strike of the Polochic fault, and their amplitude increases near the fault (Figure 6). This suggests that deformation is partitioned into N-S trending shortening and E-W trending strike-slip faulting [*Tikoff and Teyssier*, 1994]. South of the central part of the Polochic fault, NW trending folds indicate NE trending shortening, as expected from E-W trending, left-lateral shearing (Figure 6). Finally, a 120 km long E-W trending syncline, north of the Verapaz shear zone, may reflect recent activity on this structure.

[27] Geological cross sections across the Mayan paleosurface and the paleovalleys (Figure 5) show that near the Polochic fault, long-wavelength deformation has produced a major warping resulting in a kilometer-scale uplift of the Polochic fault zone relative to the center of the Polochic-Motagua sliver. Mesoscale, low-amplitude subkilometric folds affect paleoriver deposits (Figure 5). In Chicruz, recent deformation closely mimics the underlying structures, amplifies former NW trending kilometer-scale Paleocene-Eocene folds, and reactivates a SW dipping thrust. Vertical offset of the paleovalley across this reverse fault is about 200 m. A vertical slip rate of ~0.03 mm/yr is derived considering that the paleovalley is ~7 Ma old and fault motion has been constant since then. The amplitude of the paleosurface offset on the same reverse fault reaches 700 ± 100 m (Figure 6). Ascribing a middle Miocene age to the paleosurface yields a slip rate of ~0.06 mm/yr. The time-integrated velocity change indicates either a decrease of slip rate with time or a recent cessation of thrusting.

[28] Closer to the Polochic fault near Sicaché, folds associated with superficial north dipping thrusts affect the paleoriver deposits and interlayered volcaniclastic units (Figure 5, site 3 in Figure 7). Theses folds are distinct from the larger Paleocene-Eocene structures, some of which have not been reactivated since 7 Ma (cross section C, Figure 5). Deformation partitioning close to the fault may explain that in this area deformation activates both E-W folds and E-W strike-slip faults.

[29] The ~500 ka old valley of the Cahabón River has been disrupted vertically by two major normal faults bounding a horst structure (Figures 2 and 5). Horizontal kilometer-

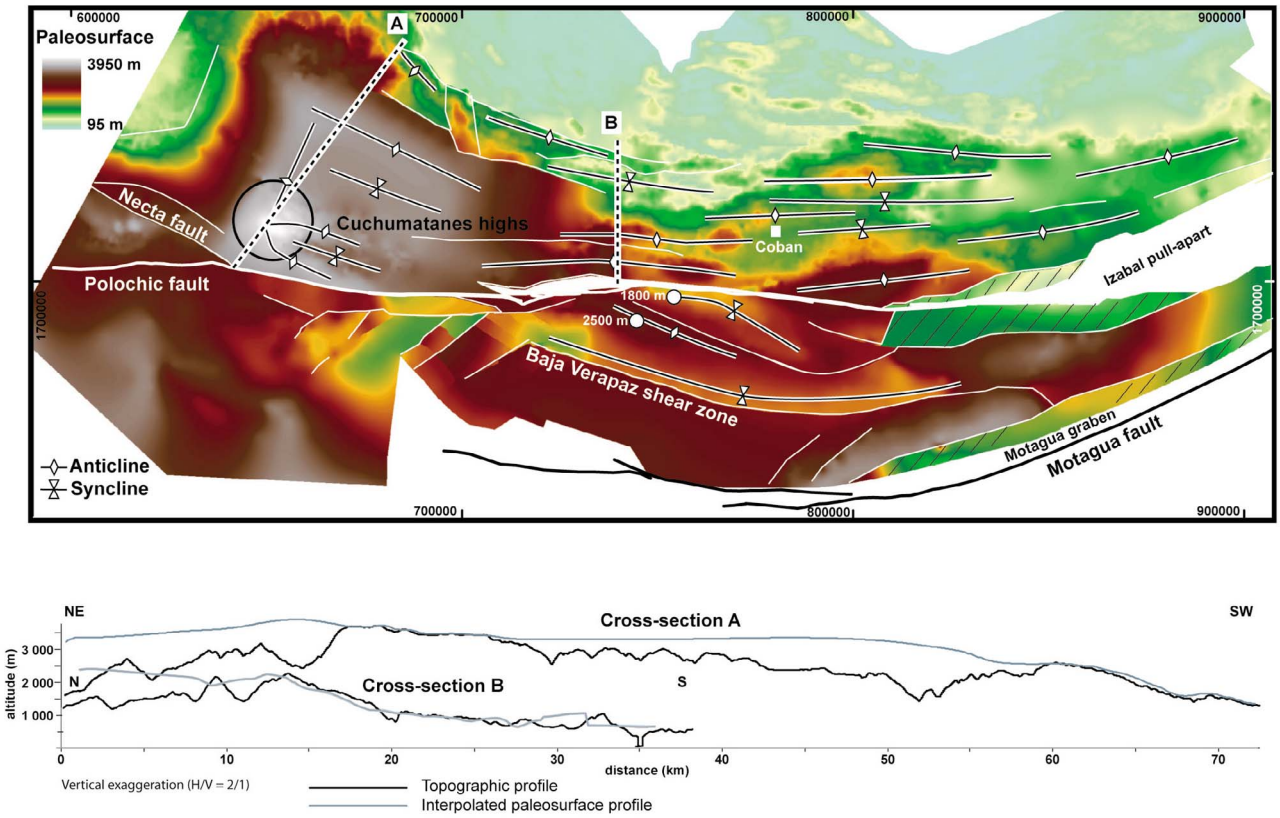

Figure 6. (top) Reconstruction of the middle Miocene paleosurface by interpolation of preserved remnants. Fold traces and faults affecting the paleosurface are shown. Dashed zones represent unreliable reconstruction due to sparse tectonic data. White circles with paleosurface elevation used to determine tectonic offset of reverse fault between two points. Black circle shows the maximum uplift of the paleosurface at the intersection between the Necta fault and the Polochic fault. Dashed black lines on a white background color indicate locations of cross sections A and B. (bottom) Cross sections A and B are associated with the topographic profiles shown in black line, and the interpolated paleosurface profiles shown in gray line, allowing calculation of the crustal shortening north of the Polochic fault.

scale sinistral valley offsets across these faults suggest contemporary horizontal slip (Brocard et al., submitted manuscript, 2011) (Figure 2). Vertical offsets reach ~80 m (cross section A, Figure 5). Analysis of fluvial deposit architecture on outcrops and by electrical resistivity tomography shows that the faults were already in motion at the time of sedimentation, prior to valley abandonment (Brocard et al., submitted manuscript, 2011). Fault motions generated block-wide uplift of an intervening horst without significant tilting, at an integrated slip rate of ~0.16 mm/yr since 500 ka. Deformation of the Mayan paleosurface is not homothetic. Actually, across the northern normal fault, paleosurface displacement remains limited, within the uncertainties of paleosurface elevation (±100 m), that is no more than paleovalley offset. This implies that the northern normal fault was activated only recently. Paleosurface vertical offset across the southern fault reaches 500 ± 100 m. Ascribing a middle Miocene age to the paleosurface yields a maximum slip rate of 0.04 ± 0.01 mm/yr. This is lower than the Quaternary slip rate deduced from the offset of the paleovalley (~0.16 mm/yr), which indicates that the velocity of the southern normal fault has increased over time. The evolution of slip rates on both faults suggests a recent expansion of the extensional regime in the Cahabón valley. Earlier inception of the extensional regime along the southern fault can be explained by its more favorable orientation. Its NE-SW strike is compatible with transtensional faulting in the context of the general E-W trending left-lateral shearing of the Polochic-Motagua sliver, even in a transpression-dominated regime. Extension along the E-W trending northern fault, however, requires the shift to a transtensional regime in the tectonic sliver.

[30] South of the Cuchumatanes Highs, the Polochic fault splays to the SW and WSW along NE to ENE trending normal faults that considerably down throw the topography (Figure 2). This extensional horsetail termination mirrors a compressional horsetail north of the Polochic fault. The normal faults displace both the paleovalleys (~7 Ma) and the Mayan paleosurface (cross sections D and E, Figure 5). Fault dips are unknown, but by assuming a 50–80° dip range, the faults can produce the observed paleosurface deformation under 700–1700 m of total extension. Normal faults have equally tilted both markers, indicating that deformation began after emplacement of volcaniclastic units in paleovalley (~7 Ma).

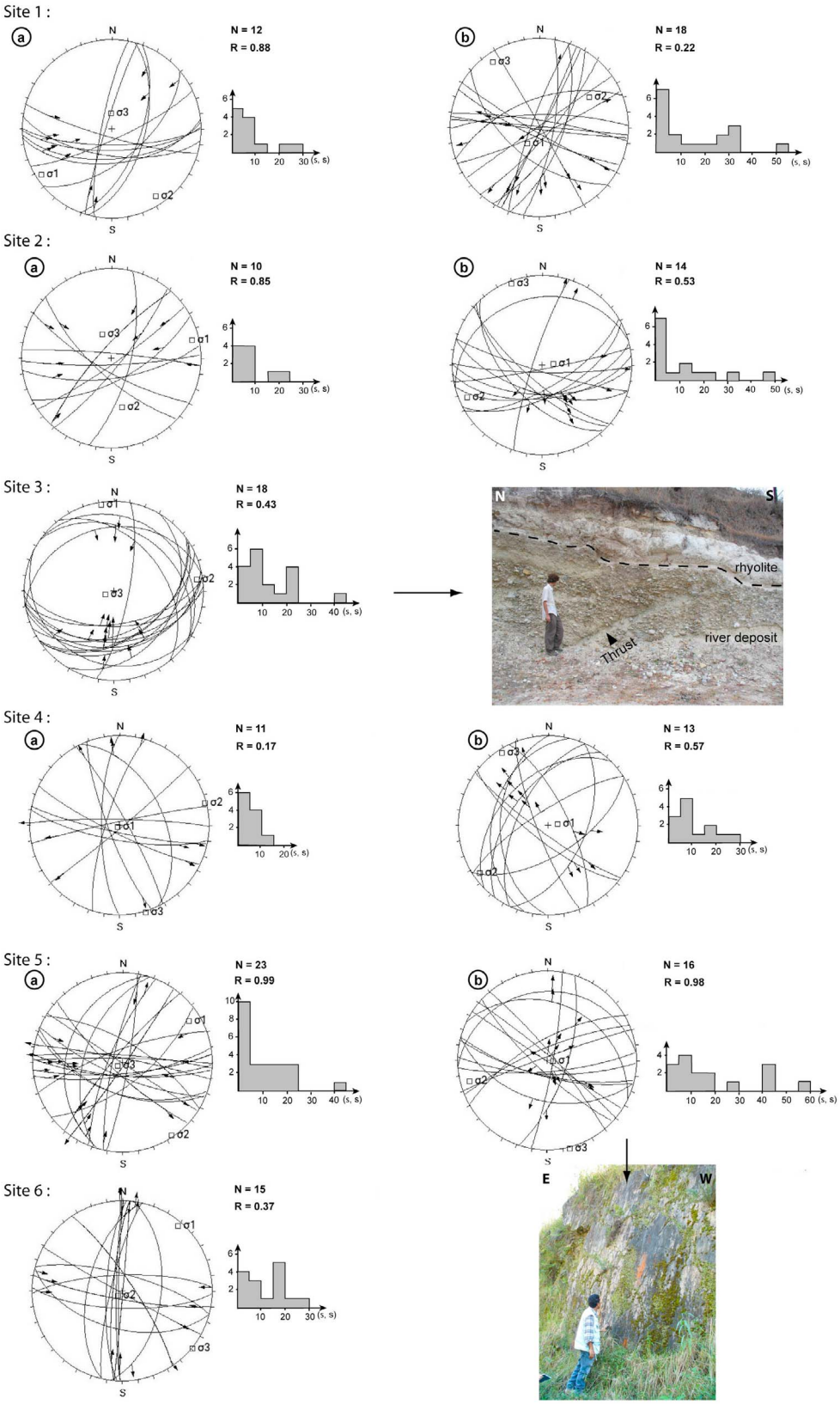

Figure 7. Fault populations and inversion results (equal angle, lower hemisphere stereonets). Sites located in Figure 2. Circled a and b indicate relative chronology of fault slip data sets. N and R give number of computed striations and stress ratio, respectively. Histograms show angular deviation (in degrees) between striation and computed shear stress for each fault. Fault inversion results of sites 3 and 5 are accompanied by the picture of representative fault of each site.

Table 1. Results of Stress Tensor Inversion From Fault Slip Data[a]

Site	X	Y	Age and Rock Type	σ_1		σ_2		σ_3		R
				Azimuth	Plunge	Azimuth	Plunge	Azimuth	Plunge	
1 (a)	773254	1690457	Cretaceous lim.	238	6	147	14	351	74	0.88
1 (b)	773254	1690457	Cretaceous lim.	225	65	55	24	324	4	0.22
2 (a)	793107	1676367	Cretaceous lim.	75	5	169	34	337	55	0.85
2 (b)	793107	1676367	Cretaceous lim.	70	81	248	8	338	0	0.53
3	731237	1688480	Miocene congl.	350	0	80	9	260	80	0.43
4 (a)	795620	1686815	Permian lim.	276	86	73	3	164	1	0.17
4 (b)	795620	1686815	Permian lim.	65	82	237	7	327	1	0.57
5 (a)	785439	1696144	Permian-Cretaceous lim.	55	8	146	3	257	81	0.99
5 (b)	785439	1696144	Permian-Cretaceous lim.	71	85	256	4	166	0	0.98
6	803632	1667100	Quaternary congl.	38	5	248	83	129	3	0.37

[a]Sites are located on Figure 4 and the corresponding strereograms on Figure 8. Letters in parentheses indicate relative chronology of distinct fault slip data populations. Lithologies are abbreviated as follows: lim., limestone; congl., conglomerate; n is the number of measurements for each site.

[31] In summary, geologic and geomorphic markers indicate that deformation between the Polochic and Motagua faults was transpressional in the late Miocene and resulted in a kilometer-scale uplift of the Polochic fault zone with respect to the Polochic-Motagua sliver interior. Away from the fault, transpression reactivated Paleocene-Eocene thrusts and folds. Closer to the fault, deformation was partitioned between strike slip on the Polochic fault and N-S shortening on E-W striking structures. Late Miocene transpression was replaced by an extensional regime that is propagating throughout the Polochic-Motagua sliver. We show hereafter that the processing of fault slip populations is consistent with the deformational evolution inferred from large-scale deformations.

4.1.4. Fault Kinematics and Paleostress Regimes

[32] We reconstructed stress tensors based on fault striations by inverting fault slip population data at six sites inside the PMFS (Figures 4 and 7). Inversions were calculated by a computer program that uses the numerical method of *Carey* [1979]. Inversion results (Table 1) yield the orientation of the principal stress axes of the computed stress tensor (σ_1, σ_2, σ_3) and the stress ellipsoid shape parameter $R = (\sigma_2 - \sigma_1)/(\sigma_3 - \sigma_1)$, which varies from 0 to 1.

[33] Fault populations were divided into homogeneous subsets by analyses of fault planes and striae orientations, and each subset was used for the calculation of a distinct tensor [*Mercier et al.*, 1991; *Bellier and Zoback*, 1995, and references therein]. We have identified two distinct families of striae at 4 of the 6 sites, generated by two slip episodes (Figures 4 and 7). Discrimination of fault populations is based on crosscutting relationships observed on the fault planes and on the numerical check for compatibility of striae with respect to a given stress state. Different stress tensors obtained by this method at any given site indicate important changes in the stress regime.

[34] Along the west to WNW trending faults at sites 1 and 2 (Figures 4 and 7), a transpressional regime ($R1_{s1}$) with ENE trending σ_1 predates an extensional regime ($R2_{s1}$) with a NNW trending σ_3. At site 1, fault slip data were collected on the WNW trending tectonic contact between Cretaceous limestone and serpentinite (Figure 4). Consequently, the age of the two stress states is younger than ophiolite obduction at 70 Ma [*Brueckner et al.*, 2009]. The tectonic contact is correlatable laterally with the thrust that offsets the paleovalley of Chicruz (cross section B, Figure 5). Stress state $R1_{s1}$ is compatible with such reverse faulting, and therefore likely mid- to late Miocene in age.

[35] At site 3 further west, an early thrust fault regime $R1_{s3}$ with north trending σ_1 is identified within 7.4 Ma old river deposits (Figures 4 and 7). Azimuth of σ_1 (N350) differs from that of $R1_{s1}$ (N238) and $R2_{s1}$ (N75), but is in agreement with E-W folding of the paleosurface north of the Polochic fault (Figures 4 and 7). Because site 3 is closer to the Polochic fault, we suspect that partitioning of the transpressional deformation into N-S shortening and E-W strike-slip faulting is taking place. Inversion of the first family of fault slip data $R1_{s5}$ at site 5, along the Polochic fault (Figures 4 and 7), indicates strike-slip faulting with σ_1 trending NE. The early fault families at sites $R1_{s1}$, $R1_{s2}$, $R1_{s3}$ are thus compatible with our earlier finding of a general transpressional regime partitioned only in the vicinity of the Polochic fault, as is also inferred from the deformation of geologic markers (cross section C, Figure 5 and Figure 6).

[36] A general change to a younger extensional stress state is identified at sites 1, 2, 4, and 5 (Figures 4 and 7). These sites share a common NNW trending σ_3, consistent with the conclusions drawn from the structural study. The similarity suggests that the current extensional stress field extends over most of the length of the Polochic fault and to the nonmetamorphic belts south of the fault. Fault kinematics matches the regional deformational history inferred from our study of geologic and geomorphic markers and is also consistent with earlier fault kinematic analyses [*Ratschbacher et al.*, 2009].

[37] At site 6, inversion of striae in Quaternary river deposits on top of the Baja Verapaz Shear Zone (Figures 4 and 7) results from a modern left-lateral strike-slip regime associated with NE trending σ_1, in agreement with the present-day kinematics of the Motagua fault [*Lyon-Caen et al.*, 2006].

4.2. Deformation North of the Polochic Fault

[38] In NW Guatemala, the Polochic fault splays toward the northwest and connects with the Tonala and Necta faults (Figure 8) [*Carfantan*, 1976; *Burkart*, 1978; *Anderson et al.*, 1985]. The two splays bound to the SW the Sierra Madre de Chiapas batholith and Cuchumatanes Highs, respectively.

4.2.1. Kinematics of the Tonala Fault

[39] West to the Polochic fault, in the Pacific shelf zone, seismic reflection profiles do not reveal any offshore continuation of the Polochic fault [*Keppie and Morán-Zenteno*,

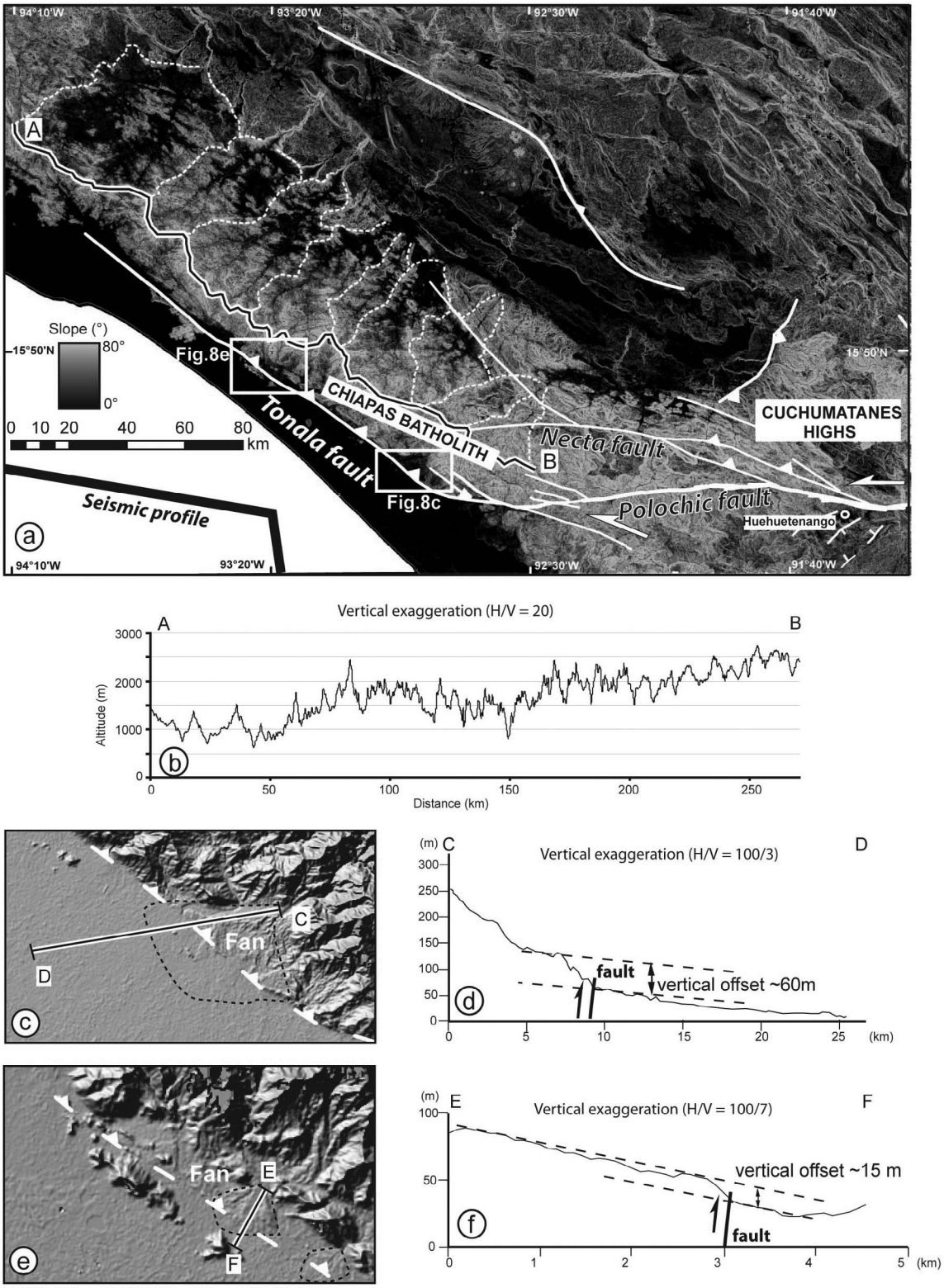

Figure 8. Tectonic study of Tonala fault. (a) Slope map in degree with fault traces locate the Figures 8c and 8e. Black and white line indicates location of topographic profile AB along the crest of the batholith. Dashed white lines show the boundaries of valleys draining toward the plate interior. (b) Topographic profile AB. (c and e) Shaded relief images of alluvial fans affected by the Tonala fault. Dashed black lines show the fan boundaries. (d and f) Cross sections CD and EF, respectively, showing vertical fan offsets due to Tonala fault activity.

2005] (Figure 8). The Tonala fault is the westernmost relay of the Polochic fault. Change in fault strike, and transfer of slip to this northern splay, with a bend opposite to plate motion, must induce shortening. A topographic profile following the crest of Chiapas batholith (profile AB, Figure 8) exhibits an along-strike increase in altitude toward the inside corner of the junction of the Polochic and Tonala faults, as expected in a restraining bend. There, valleys are deeply incised. Since precipitations do not vary significantly along the Sierra Madre (http://www.atmosfera.unam.mx/uniatmos/atlas/uniatmos_eng.html), deeper incision can be interpreted as an erosional response to enhanced surface uplift within the inside corner. Valleys of the Sierra Madre draining toward the plate interior widen and flatten away from the corner (Figure 8a), suggesting that the landscape has entered a phase of postuplift relaxation, following a temporal decrease of incision.

[40] Tectonic landforms compatible with active reverse faulting are recognized along the Tonala fault, such as offset alluvial fans and fault scarps. Two recent alluvial fans are displaced vertically by 60 m and 15 m, respectively, the first near the connection between the Tonala and the Polochic faults and the other 60 km further northeast (Figures 8c, 8d, 8e, and 8f). The Sierra Madre de Chiapas relief is asymmetric, with a gentle NE side and a steep SW flank bordered by the Tonala fault (Figure 8). Vertical motion along the Tonala fault may have produced the tilting of the range and generated this asymmetry. No active strike-slip motion is detected in the morphology, whereas strike-slip mylonitization occurred extensively along the Tonala fault in the late Miocene [*Wawrzyniec et al.*, 2005; *Ratschbacher et al.*, 2009].

4.2.2. Growth of the Cuchumatanes Highs

[41] In NW Guatemala, the Cuchumatanes Highs are bounded by four major structures that delineate a trapezoidal plateau: the Polochic fault and the Necta fault to the south [*Anderson et al.*, 1973]; a NNE-SSW reverse fault to the west; the Chiapas fold-and-thrust belt to the north; and several E-W to NW-SE reverse faults to the NE (Figure 2). Surface uplift of the middle Miocene paleosurface in the plateau exceeds 3000 m (Figure 6). Uplift was produced by the conjunction of four processes associated with 3 shortening directions (~N00, ~N50, and ~N110):

[42] 1. An E-W range runs along the northern side of Polochic fault. It is composed of E-W trending folds and is bounded to the north by major E-W trending reverse faults [*Franco et al.*, 2009]. These structures are generated by ~N00 shortening and were first active in Paleocene-Eocene time [*Anderson et al.*, 1973; *Walper*, 1960]. The faults were beveled when the Mayan paleosurface formed and have been reactivated since the middle Miocene (Figure 6). Approximately N00 shortening may result from strain partitioning of the convergence vector, which is oblique to the Polochic fault according to GPS vectors north to the fault [*Lyon-Caen et al.*, 2006; *Rodriguez et al.*, 2009].

[43] 2. To the NE of Cuchumatanes Highs, the frontal thrusts bend from E-W to NW-SE as they approach the Chiapas belt (Figure 2). This change of strike could be a result of the interaction between the Chiapas ~N50 shortening and the partitioning described above.

[44] 3. To the SW of the Cuchumatanes Highs, change of strike and slip transfer from the Polochic fault to the Necta fault are expected to induce transpression along the Necta fault (Figure 2). *Anderson et al.* [1973] indicate oblique slickensides along the Necta fault. Such a transfer would account for the locus of the maximum paleosurface uplift of 3500 m in the fault bend (cross section A, Figure 6).

[45] 4. To the West, ENE-WSW thrust and associated folds bound the highs and interact with NW-SE folds of the second and third groups described above (Figure 6). The ~N110 shortening necessary to produce these structures is a key element that will be addressed in the discussion.

[46] We use the uplift of the Mayan paleosurface to estimate the total finite shortening necessary to form the Cuchumatanes Highs. Two cross sections are drawn perpendicular to the structures (cross sections A and B, Figure 6). The first section crosscuts the E-W trending range and documents the uplift produced by ~N00 shortening due to partitioning of the convergence vector. The second cross section traverses the Cuchumatenes Highs through the inner corner of the bend that connects the Necta and Polochic faults.

[47] The thickness of lithosphere involved in the shortening is unknown, so only end-member scenarios are considered. If deformation results from buckling only, a simple line length balancing of the paleosurface provides a minimum value of finite shortening: 1.4 km along the N-S section A, and 1.7 km in the inner corner along section B; this corresponds to shortening rates of 0.14 and 0.17 mm/yr for a minimum paleosurface age of 10 Ma. In the other end-member model, deformation involves the entire crust and is locally compensated (Table 2). We assume that before 10 to 17 Ma, topography was flat and near sea level [*Brocard et al.*, 2011]. Both the modern topographic profile and the paleosurface profile are used to calculate the total cross-sectional area below the two profiles and above sea level. The corresponding area of isostatically compensated lithospheric root is calculated using crustal and lithospheric mantle densities of 2700 and 3300 kg/m^3, respectively [*Turcotte and Schubert*, 2002; *Hoke and Garzione*, 2008]. Crustal thickness under cross section B (Figure 6) ranges from 35 to 40 km according to a seismological study [*Franco et al.*, 2009] and from 35 to 50 km (cross section A, Figure 6) west of the highs according to the high negative Bouguer gravity anomaly that is localized on the Cuchumatanes Highs. The trapezoid shape of the anomaly mimics the topographic shape of the Highs, suggesting local compensation [*Burkart and Self*, 1985]. We then combine these values with the area of the compensated lithospheric root estimated from the topography and the paleosurface profile to calculate a range of finite crustal shortening values (Table 2). A ~N50 shortening rate of 1 to 3.2 mm/yr is found in the Cuchumatanes inner bend, and a ~N00 shortening rate of 0.3 to 0.7 mm/yr is calculated in the E-W range, for deformation starting between 17 and 10 Ma (Table 2). These values of shortening are not very high, but uplift/shortening rates could be higher if tectonic activity started or accelerated more recently than 10 Ma, as suggested by the extensive preservation of the uplifted paleosurface.

4.3. Deformation Along the Guatemala Volcanic Arc

4.3.1. Kinematics of the Jalpatagua Fault

[48] In SW Guatemala (Figure 2), the volcanic arc is affected by the right-lateral, trench-parallel strike-slip Jalpatagua fault [*Wunderman and Rose*, 1984]. The fault isolates

Table 2. Crustal Shortening Estimates North to the Polochic Fault[a]

	Crustal Thickness 35 km				Crustal Thickness 50 km			
	Topography		Paleosurface		Topography		Paleosurface	
Deformation Age	Shortening (km)	Shortening Rate (mm/yr)	Shortening (km)	Shortening Rate (mm/yr)	Shortening (km)	Shortening Rate (mm/yr)	Shortening (km)	Shortening Rate (mm/yr)
				NE-SW Trending Cross Section A				
10 Ma	25.1	2.5	31.9	3.2	17.6	1.8	22.3	2.2
17 Ma	25.1	1.5	31.9	1.9	17.6	1	22.3	1.3
				E-W Trending Cross Section B				
10 Ma	5.4	0.5	7.3	0.7	4.8	0.5	6.4	0.6
17 Ma	5.4	0.3	7.3	0.4	4.8	0.3	6.4	0.4

[a]Finite shortening and shortening rate necessary to uplift the paleosurface and generate the topography represented in the cross sections A and B of the Figure 6 are calculated taking a purely crustal shortening approach [*Turcotte and Schubert*, 2002; *Hoke and Garzione*, 2008].

a fore-arc sliver alongside the Cocos-Caribbean subduction trench, named the Central American fore-arc sliver [*DeMets*, 2001]. The location, strike, and displacement along the fault likely result from the combination of three factors: lithospheric mechanical weakening along the volcanic arc, eastward drift of the Caribbean plate, and low degree of interplate coupling along the Pacific subduction [*Lyon-Caen et al.*, 2006; *Álvarez-Gómez et al.*, 2008]. The low degree of coupling can be a consequence of slab geometry and/or relative motion [*Heuret and Lallemand*, 2005] between the Caribbean and Cocos plates [*Álvarez-Gómez et al.*, 2008]. The fault affects Quaternary volcanic deposits [*Wunderman and Rose*, 1984; *Duffield et al.*, 1992].

[49] South of Guatemala City, the Los Esclavos River and its alluvial fan are affected by the fault (Figure 9). The river is laterally offset by 6.5 to 8.7 km, the width of the valley being the source of uncertainty. The fault also displaces the apex of an alluvial fan (Figure 9). To measure the fan offset with respect to its feeder valley, the location of the fan's apex was reconstructed using the intersection point of the streambeds that radiate over the surface of the fan (Figure 9b). Location uncertainty is 400 m, so the measured tectonic lateral offset of the fan is 1.2 ± 0.2 km. Inversion of our fault slip measurements in Quaternary volcanic deposits yields a NW trending σ_1, oriented 10° clockwise of the fault strike (Figure 9c). This orientation is consistent with right-lateral strike slip on the fault and with the strain field predicted by *Rodriguez et al.* [2009] in this area.

4.3.2. Tectonic Style Between the Tonala and the Jalpatagua Faults

[50] The Jalpatagua fault terminates near the Pacaya volcano (Figure 10). Some other trench-parallel right-lateral faults are suspected in its continuation, inside the caldera of Amatitlan, and within a NW trending graben of its resurgent dome [*Wunderman and Rose*, 1984]. The downfaulted area is older than the caldera (of maximum age 300 ka), so the Jalpatagua fault may be masked by younger volcanic activity. The three nested calderas of Lake Atitlan range in age from 14 Ma to 84 ka (Figure 10) and are affected by well-defined NW and NE trending faults displaying right- and left-lateral slip, respectively [*Newhall*, 1987]. We conclude that trench-parallel dextral faulting continues along the volcanic arc from the Jalpatagua fault up to the area where the Motagua fault dies out near Chichicastenango (Figure 10). This is in agreement with the occurrence of strike-slip focal mechanisms up to this area (Figure 2).

[51] No more evidence of dextral motion is found NW of the Atitlan calderas and the western termination of the Motagua fault. Some trench-parallel faults have been described by *Mora et al.* [2004] and *Van Wyk de Vries et al.* [2007] north of the Tajamulco and Tacana volcanoes, but their kinematics are not reported. South of the Tonala fault, a well-expressed trench-parallel fault straddles the NW region of the Tacana volcano and connects to the Tonala fault. The zone between the Atitlan and the Tacana volcanoes is a rather rolling topography standing at high elevation, with basement rocks reaching 3500 m (Figure 10). The central flat and high area is bounded on both sides by major trench-parallel topographic lineaments (Figure 10a). This axial high drops by 1000 m south to the Atitlan caldera (Figures 10b and 10c). Uplift is thus restricted to a trench-parallel faulted zone that links the Jalpatagua fault–Motagua fault terminations to the Tonala fault southern termination. This uplift is likely related to a relay zone and a restraining bend at the western termination of the Motagua fault [*Rodriguez et al.*, 2009]. Next to this high, the fore-arc sliver is a low standing, continuous block bounded by the Jalpatagua fault, the relay zone, and the Tonala fault. Large magmatic bodies intruded along this relay zone during Quaternary time [*Newhall*, 1987]. They may affect the rheological properties of the crust, producing wide ductile transpressional deformation in the lower crust and distributed uplift at the surface, instead of a sharp, continuous fault trace. Furthermore, long-term finite deformation is largely obliterated by recent (<100 ka) and thick (>200 m) volcanoclastic aprons. GPS measurements [*Lyon-Caen et al.*, 2006] in this zone image a dim velocity gradient compatible with left-lateral motion, though it remains in the reported velocity uncertainties of 4 mm/yr (±2 mm/yr error ellipses).

5. Discussion

[52] The current NACC triple junction is diffuse and involves major faults and continental blocks with different kinematics. We propose two genetic models that explain our own observations about the modern tectonic setting and earlier observations largely described in previous studies. Meanwhile these models pursue a larger goal because they

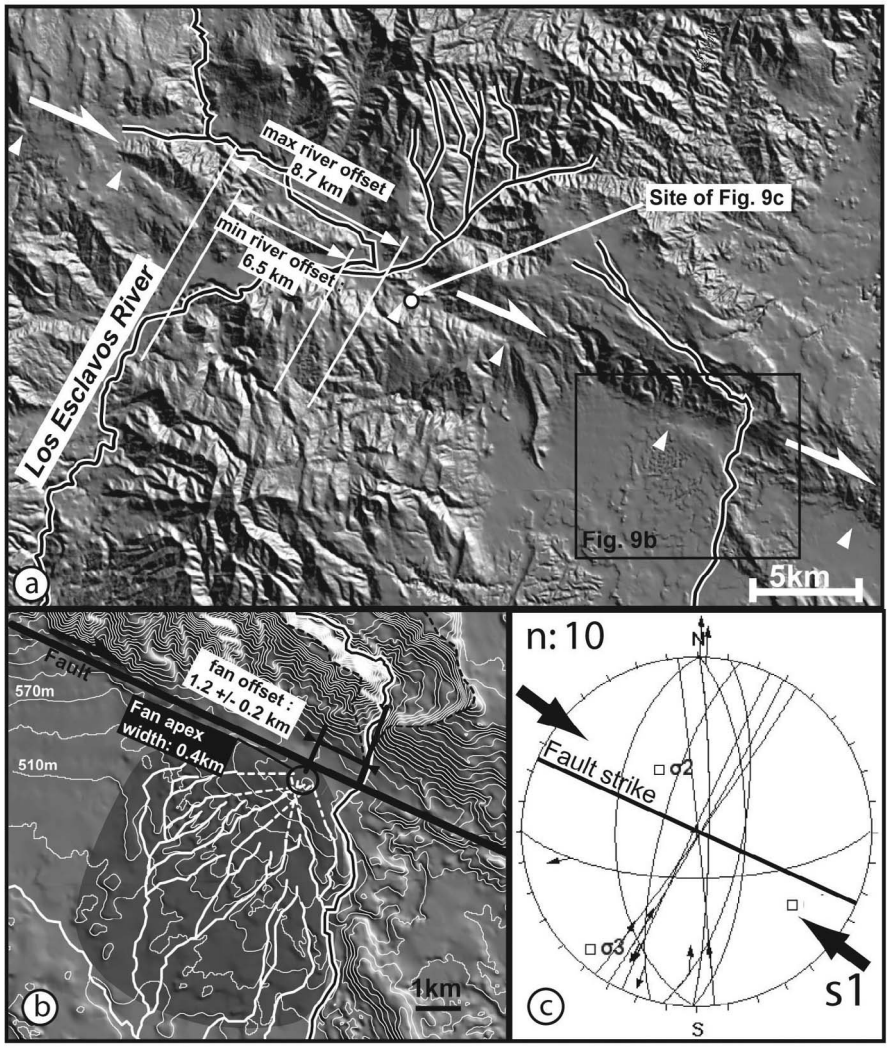

Figure 9. Evidence of the Jalpatagua fault activity. (a) Shaded relief map shows drainage pattern and relation to fault. Fault trace is indicated by white triangles. Minimum and maximum lateral offsets of the Los Esclavos river are represented taking into account the uncertainties produced by the width of the valley. (b) Shaded relief map with superimposed 30 m contours (thin white lines) focused on the studied alluvial fan (gray surface). Black dashed lines indicate the boundaries of the feeder valley. White lines on the alluvial fan correspond to the streams incising the fan. White dashed lines show the strikes of the drainage extended upward. This drainage was extracted from ASTER DEM (30 m resolution) and Landsat satellite images. They allow location of the fan apex indicated by a black circle. The distance between the fan apex and the source valley represents the lateral fan offset. (c) Fault populations and inversion results obtained on a site located on the Jalpatagua fault trace; n is the number of fault slip data. Location is shown on Figure 2.

also account for the tectonic evolution of the PMFS during the entire Neogene, the motion of the Chortís block, the lack of torsion of the Cocos slab at the triple junction, and the existence of a fossil strike-slip fault along the coast of Mexico. The two models must be combined and integrated with earlier models to explain the kinematic evolution of the NACC triple junction. We present them separately first, and discuss their merit in view of the regional geology, before integrating them into a single progressive model of triple junction evolution that can be transposed to other regions.

5.1. "Pull-Up" and "Zipper": Kinematic Models of Triple Junction Migration

[53] In the case of a triple junction composed of an oceanic plate subducted below two continental plates, with the continental plates bounded by a transform margin, transform motion induces lateral offset of the trench and thus tends to twist the slab [*McKenzie and Morgan*, 1969]. If the slab does not twist because of its internal strength or because it is strongly coupled to the mantle, the overlying continental plates must accommodate deformation. Accommodation by

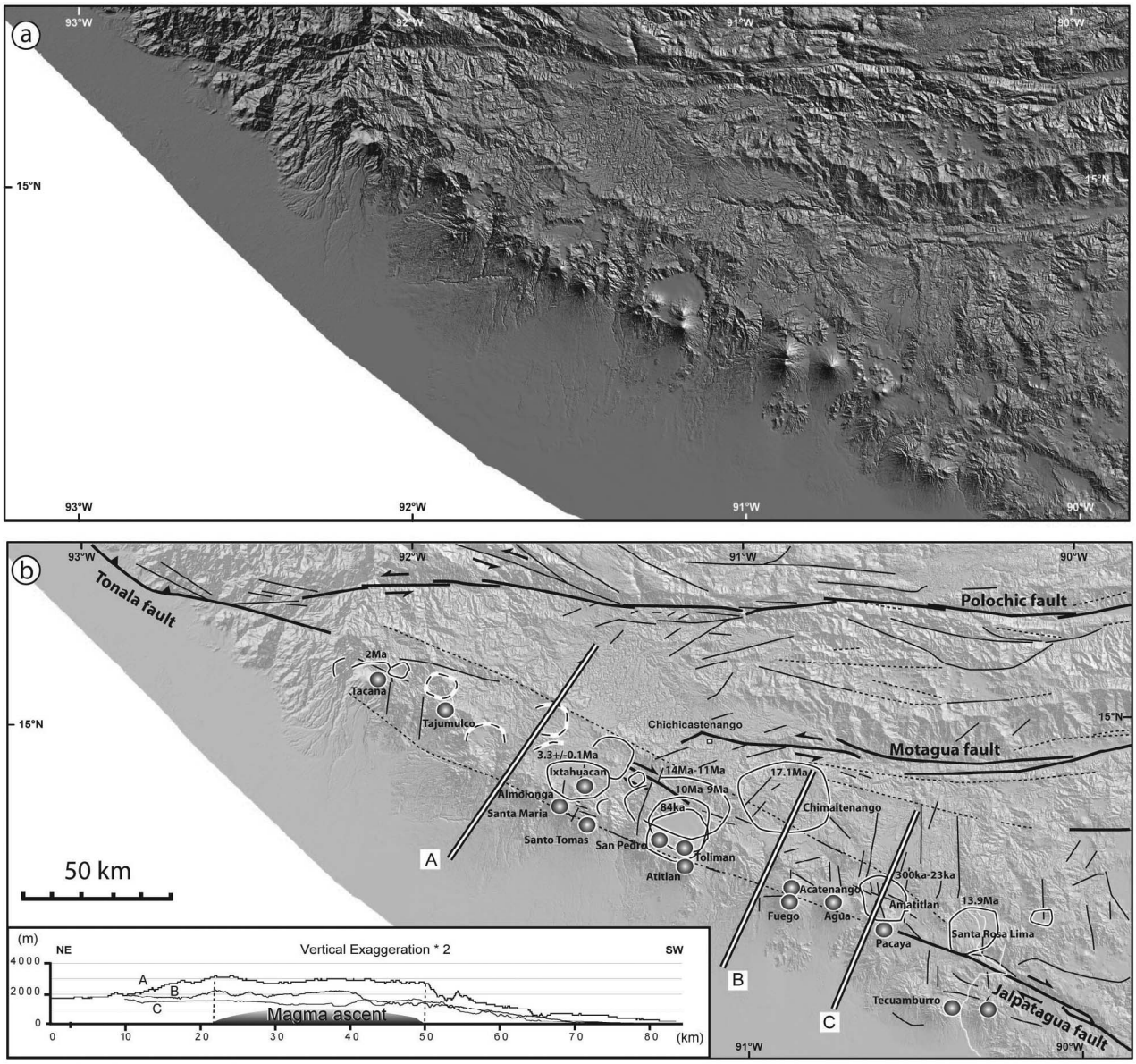

Figure 10. Fault segmentation and volcanism of western Guatemala. (a) Shaded relief image of the volcanic arc and the western tip of the Motagua fault. (b) Fault segmentation, volcanism of the western Guatemala. Calderas described in the references are shown as white and black circles; supposed calderas are shown by dotted black and white circles. Stratovolcanoes are named and represented by white and black points. White fine line in the southeastern wedge of the image corresponds to the Los Esclavos river offset by the Jalpatagua fault. Ages of calderas come from *Newhall* [1987] and *Rose et al.* [1987] for the Atitlan calderas and Chimaltenango and Ixtahuacan calderas, from *Reynolds* [1987] for the Caldera of Santa Rosa Lima, from *Wunderman and Rose* [1984] for the caldera of Amatitlan, and from *García Paloma et al.* [2006] for the Tacana volcano. Topographic profiles A, B, C are located in the shaded relief image of Figure 10b and presented in the inset.

overriding plate is common in subduction zones, for example in response to the subduction of oceanic plateaus or seamounts [*Dominguez et al.*, 1998; *Sallarès and Charvis*, 2003]. In the present case, shortening in one upper plate and extension in the other upper plate accommodate the differential plate motion and preserve the linearity of the trench [*Phipps Morgan et al.*, 2008]. However, such diffuse intraplate deformation is not permanently sustainable. Other processes concur to accommodate space, and two such processes of accommodation are discussed here, the "pull-up" process and the "zipper" process (Figure 11).

[54] The "pull-up" process consists of taking off a block of the plate that converges toward the subduction zone, and displacing this block toward the retreating upper plate (step A, Figure 11a). The new block is delimited by the subduction zone on one side and by a new strike-slip fault on

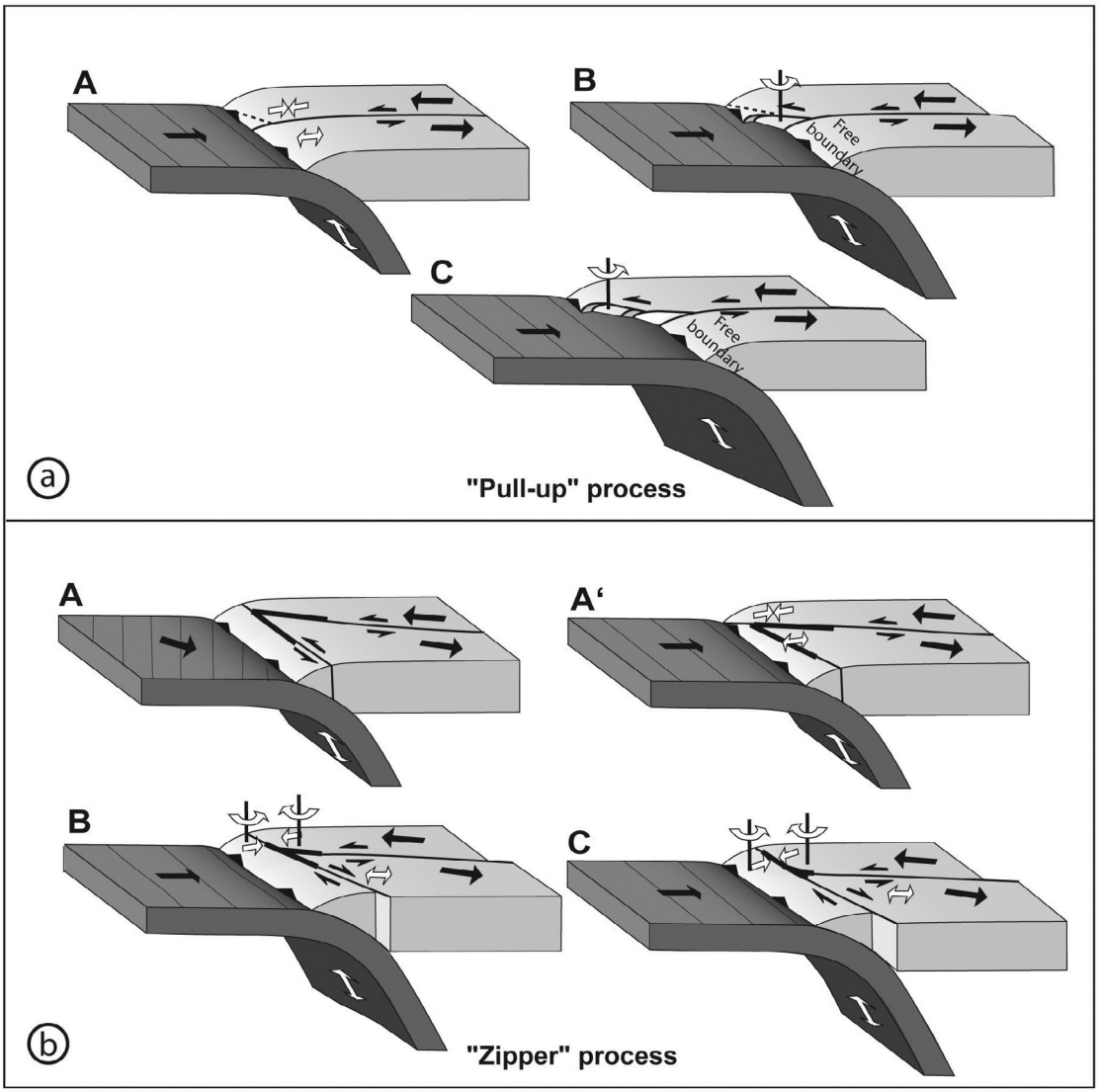

Figure 11. Two general models of kinematic evolution of triple plate junction. (a) Steps A to C show the "pull-up" process associated with the detachment of blocks of the upper plate converging toward the subduction zone to be integrated in the kinematics of the upper plate diverging from the subduction zone. Linear white arrows indicate stretching. Face to face white arrows indicate shortening. Black lines represent the gravity anomalies formed within the oceanic plates. (b) Steps A to C show the "zipper" process implying the zipping of the transform boundary with the conjugated fault that bounds the fore-arc sliver in the upper plate diverging from the subduction zone. Steps A and step A′ show the different solution to generate a fore-arc sliver. Step A induces partitioning of the oblique convergence; step A′ shows the model of *Phipps Morgan et al.* [2008] indicating that the fore-arc sliver is produced to compensate the relative upper plate motion and to avoid the slab torsion. Thick black portions of the dextral and sinistral faults indicate the "zipper" process. Small face to face or opposite arrows indicate shortening and extension, respectively.

the other side (step B, Figure 11a). Some rotation occurs during block motion in order to adjust the strike of the block to the trend of the transform boundary. A series of blocks can be generated successively as transform displacement increases (step C, Figure 11a). This process reduces the lateral offset between the overriding plates and helps reduce twisting of the slab. Blocks from one plate are dragged in the transform zone because retreat of the other plate creates a "free" boundary next to the triple junction (Figure 11a). The process can eventually lead to a complete transfer of the pulled up blocks into the trailing edge of retreating plate.

[55] The "zipper" process involves a fore-arc sliver (Figure 11b). The fore-arc sliver can be first generated by strain partitioning of the oblique convergence of the subducted plate into the overriding plates [*Fitch*, 1972; *McCaffrey*, 1992; *Teyssier et al.*, 1995] (step A, Figure 11b). It can also be produced to accommodate the retreat of the overriding plates, next to the triple junction. Indeed, if the

subducted plate does not tear, fore-arc motion must remain continuous along the trench across the triple junction, and stretching of the overriding plate occurs behind the volcanic front [*Phipps Morgan et al.*, 2008] (step A′, Figure 11b). As differential displacement amplifies between the overriding plates, the fore-arc sliver and/or the converging upper plate must rotate about a vertical axis (step B, Figure 11b). Rigid rotation of the fore-arc sliver occurs because one part is pushed toward the trench by the trench-converging plate while the other is sucked in the wake of the escaping plate. The converging upper plate rotates if the lateral displacement of the transform boundary is transferred to the fore-arc sliver boundary. These rotations and the retreat of the diverging upper plate lead to the juxtaposition of the fore-arc sliver to the converging upper plate (steps B and C, Figure 11b). The process is amplified if the upper diverging plate is pinched and extrudes between the fore-arc sliver and the converging upper plate. A strike-slip fault, the motion of which is antithetic to the transform plate boundary, develops parallel to the subduction zone and separates the sliver from the diverging plate. As a result, the diverging plate is free to drift away from the subduction zone as a relatively rigid block (step C, Figure 11b). The antithetic strike-slip faults unite progressively like in a "zipper," leaving the fore-arc sliver stranded in front of the converging plate, while the triple plate junction migrates (steps C, Figure 11b). Henceforth, we refer to this type of closure as a "zipper" process. This process makes the triple plate junction a permanently diffuse area, and the transform boundary never joins the trench.

[56] The term "zipper tectonics" has been applied to explain (1) the progressive "zipper" closing of an ocean associated with the migration of rotational oblique collision [*Şengör et al.*, 1993; *Shelley and Bossière*, 2002] and (2) the extrusion of continental blocks in a context of continental collision with the help of one major curved strike-slip fault [*Leloup et al.*, 2001]. To our knowledge, the "zipper tectonics" process proposed here has never been used to describe the evolution of a triple junction with a subduction zone coming across a continental transform boundary. In this case, "zipper tectonics" implies the existence of a fore-arc sliver and progressive suturing of the transform boundary, with a conjugate trench-parallel fault bounding the sliver. This mechanism is potentially important because it may explain the juxtaposition of oceanic "exotic" terranes along continental margins and the incorporation of continental slivers against oceanic plates.

5.2. The NACC Triple Junction and the "Pull-Up" Model

[57] North of the Polochic fault, our analyses of paleosurface deformation and earthquakes focal mechanisms [*Cáceres et al.*, 2005] document a complex compressional regime that uplifts the Cuchumatanes Highs. We have distinguished three different directions of shortening: N-S, NE-SW and WNW-ESE. N-S shortening results from partitioning of the North American plate motion with respect to the Caribbean plate, which is slightly oblique to the Polochic fault and is located there because of the buttressing effect of the fault. NE-SW shortening may have resulted, first from the Miocene Chiapas orogeny, and more recently from slip transfer along the northern splay of the Polochic fault [*Carfantan*, 1986; *Guzmán-Speziale and Meneses-Rocha*, 2000; *Meneses-Rocha*, 2001]. The WNW-ESE shortening affecting the western side of the Cuchumatanes Highs has not been interpreted. We propose that this shortening is produced by "pull-up" of a block from the North American plate. *Guzmán-Speziale and Meneses-Rocha* [2000] and *Andreani et al.* [2008] link the Polochic fault to the strike-slip faults straddling the Chiapas fold belt. These faults mark the boundaries of a continental block, named Southern Mexico block by *Andreani et al.* [2008], decoupled from the North American plate and migrating to the SE. This block takes up some of the transform plate motion and moves toward the triple junction. The kinematics of this block is compatible with the "pull-up" process described above, and its leading edge locally experiences WNW-ESE shortening as it abuts the Polochic fault.

[58] When did pulling up of the Southern Mexico block initiate? In NW Guatemala, the western tip of the Polochic fault forms a horsetail termination. Our data show that since at least the late Miocene, the Polochic fault has been transferring part of its motion to the horsetail faults to the north. The westernmost fault in the tail is the Tonala fault. Our geomorphic observations suggest active reverse motion near its connection to the Polochic fault, but some relaxation of uplift rates is observed away from the tail, close to the northern termination of the Tonala fault. This may reflect a decrease in activity away from the current location of the tail and implies that, recently, more motion has been transferred to faults located further inland, such as the Necta fault and other strike-slip faults in Chiapas [*Guzmán-Speziale and Meneses-Rocha*, 2000; *Andreani et al.*, 2008]. Witt et al. (submitted manuscript, 2011) document an age between 9 and 6–5 Ma for this slip transfer. We think that activity of these faults has generated uplift in the Cuchumatanes Highs after the middle Miocene. Displacement along the Chiapas faults marks the beginning of SE motion of the Southern Mexico block. Consequently, decrease of activity on the Tonala fault and uplift of the Cuchumatanes Highs can be correlated with the onset of motion of the Southern Mexico block (Figure 12a).

[59] We suspect that the Motagua-Polochic tectonic sliver has also been pulled up into the transform boundary. Our data show that transpressive deformation that affected the sliver, like the blocks of the North American plate, shifted to extension recently, as if extension of the Chortís block, first bounded to the north by the Motagua fault or the Jocotán-Chamelecón faults, had propagated northward up to the Polochic fault (Figure 12b). This agrees with fault kinematic data [*Ratschbacher et al.*, 2009] and suggests that the sliver, after accommodating some transform displacement for millions of years, is now being incorporated into the Caribbean realm. We suspect that some other slivers have been transferred by the same process from the southern coast of Mexico. The Las Ovejas complex with El Tambor formation, called Sula terrane by *Ortega-Gutiérrez et al.* [2007] and Copan terrane by *Flores* [2009], is a sliver of similar size, bounded by the Motagua and the Jocotán-Chamelecón faults. It has been accreted to the nuclear Chortís block in the strictest sense. The Chortís block, in turn, was stripped off southern Mexico. The successive transfer of these blocks to the Caribbean plate along the transform margin implies a migration of the NACC triple

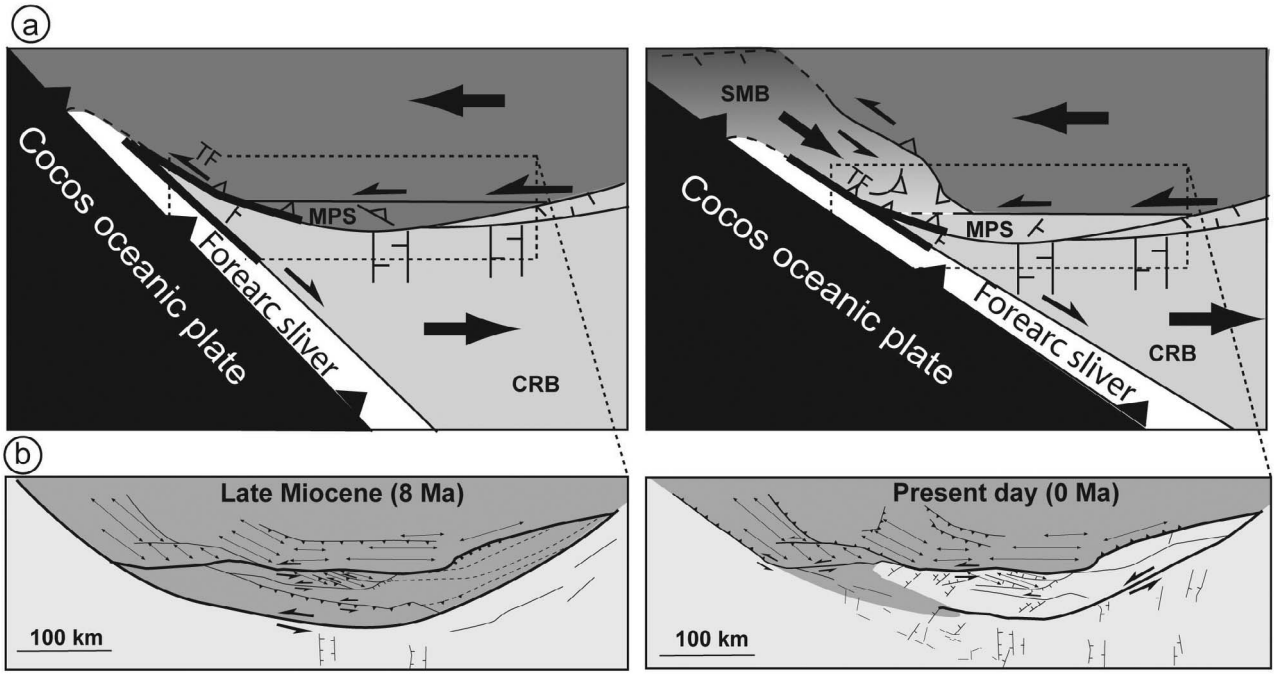

Figure 12. Two-stage model of late Cenozoic evolution of NACC triple junction migration and its northern transform boundary. (a) North America plate dynamics zone is indicated in dark gray, and Caribbean plate dynamics zone is indicated in light gray. Thick black portions of the dextral and sinistral faults indicate the "zipper" process. CRB, Chortís rift block; MPS, Motagua-Polochic sliver; SMB, Southern Mexico block; TF, Tonala fault. (b) Enlargement around the PMFS. Compressional zone is indicated in dark gray; extensional zone is indicated in light gray.

plate junction with time, helps avoid slab torsion, and accommodates diffuse motion in the overriding plate in the vicinity of the triple junction.

[60] The "pull-up" process may have also operated at the multiple plate junction between the Caribbean, South American, Cocos, and Nazca plates. The northwestern part of the South American plate is broken into a series of blocks, such as the Cordillera Oriental–Upper Magdalena block, the Cordillera Central-Middle Magdalena block, and the Maracaibo block. These blocks are pinched out by the Nazca plate convergence and dragged by the Caribbean plate eastward relative motion and therefore move toward the NNE-NE [*Taboada et al.*, 2000; *Corredor*, 2003; *Montes et al.*, 2005]. Their tectonic evolution mirrors that of the Southern Mexico block.

5.3. The NACC Triple Junction and the "Zipper" Process

[61] The fore-arc sliver is delimited by the Jalpatagua and Tonala faults, which are in perfect continuation with one another, albeit located on two opposite sides of the PMFS termination. These faults are a key element of this model and define a single fore-arc sliver of uniform width [*Phipps Morgan et al.*, 2008]. This fore-arc sliver is dissociated from the Caribbean plate by the Jalpatagua fault (Figure 13) and may have originated by strain partitioning within the Caribbean plate, above the subducted Farallon plate, when the convergence vector was more oblique than it is today [*Pindell et al.*, 2005]. It may also be a more recent feature, the movement of which preventing torsion of the Cocos slab [*Phipps Morgan et al.*, 2008]. A major observation concerning the "zipper" process is that the northernmost evidence of active dextral strike-slip faulting along the Jalpatagua fault zone coincides with the westward termination of the Motagua fault near the Atitlan calderas (Figure 10). Consequently, the Caribbean plate portion delimited by the Jalpatagua fault and the sinistral Motagua fault form a wedge-shaped region (Chortís Rift domain) [*Rogers and Mann*, 2007]. Conjugated lateral motion along the two faults allows the relative eastward motion of this zone with respect to the trench (Figure 12a). At the tip of the wedge, this motion induces extension associated with NE trending normal faults. To reduce this space, we propose that the Jalpatagua fault and the Motagua fault are zipped from the Atiltlan area up to the Tonala fault (Figure 12a). The Jalpatagua and Motagua faults are currently linked by small NE trending normal faults at the junction (Figure 10). Zipping episodes may alternate with extension to produce this diffuse connection between the faults.

[62] Zipping of the Motagua fault and the Jalpatagua fault has left a suture, which is known as the Tonala fault. The seamed fore-arc sliver, stranded along the Sierra Madre de Chiapas, forms the coastal plains between the Sierra Madre and the trench. The fore-arc sliver ends northward in the Gulf of Tehuantepec and the Tonala fault also disappears in this zone. The coastal platform reduces drastically in the bend of the trench (Figure 13). An older sinistral fault zone accommodated earlier displacements of the Chortís block. This fault is located 200 km west of the Tonala fault [*Riller et al.*, 1992; *Herrmann et al.*, 1994; *Nieto-Samaniego et al.*,

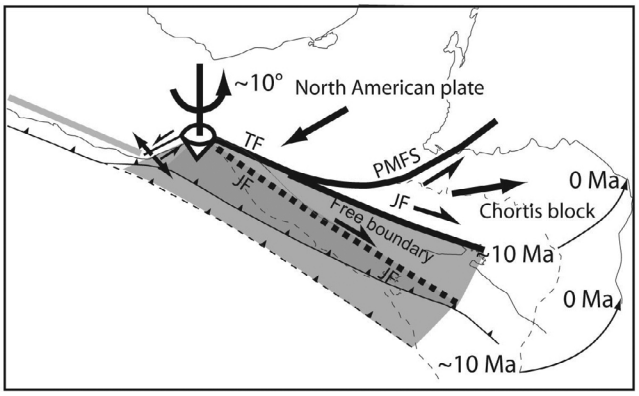

Figure 13. Late Cenozoic evolution of the fore-arc sliver of the NACC triple junction showing the "zipper" process. The fore-arc sliver is represented in gray. Fine dashed gray line corresponds to the location of the Chortís block relative to the North American plate at around 10 Ma. Fine dashed black line represents the subduction trench at 10 Ma. Bold dashed line corresponds to the fault bounding the fore-arc sliver merging with the transform boundary. The free boundary is due to the divergence of the Chortís block from the subduction zone. Fine black line corresponds to the northwestern boundary of the fore-arc sliver. Gray dashed line shows the ancient transform boundary before 10 Ma. JF, Jalpatagua fault; PMFS, Polochic Motagua fault systems; TF, Tonala fault.

2006; *Solari et al.*, 2007; *Tolson*, 2007]. We suggest that the "zipper" process began with the deactivation of this older sinistral fault zone after Oligocene time [*Tolson*, 2007], in agreement with the 10–8 Ma age of shearing along the Tonala fault that is inferred from Ar-Ar and U-Pb dating from mylonites [*Ratschbacher et al.*, 2009], and from pervasively sheared plutons [*Wawrzyniec et al.*, 2005].

[63] During the Miocene, sinistral motion along the Tonala fault accommodated the passage of the Chortís block [*Wawrzyniec et al.*, 2005; *Ratschbacher et al.*, 2009]. According to the "zipper" model, the wedge-shaped region of the Chortís block was for a time located between the coastal domain and the Sierra Madre de Chiapas (Figure 12a). Constant transform motion of 2 cm/yr over the past 10 My implies that the western tip of the Chortís block was located 200 km west of its present location 10 Ma ago (Figure 13) [*Rosencrantz et al.*, 1988; *Pindell et al.*, 2005; *Lyon-Caen et al.*, 2006]. This distance corresponds to the length of the Tonala fault, which was deactivated progressively by seaming of the Zalpatagua et Motagua faults. Therefore, the Tonala fault shear indicators should reflect this seaming and incorporate both dextral and sinistral kinematics. Indeed, *Wawrzyniec et al.* [2005] observed such combination of dextral and sinistral shear indicators in the mylonitic fabrics of the Tonala fault zone. Our geomorphological observations suggest dominant active reverse motion along the Tonala fault. Zipping explains the absence of active lateral displacement and the reverse motion occurs because it accommodates North American plate convergence toward the subduction zone and motion transfer from the E-W trending Polochic fault to the NW-SE trending Tonala fault as a strike-slip fault-bend termination [*Storti et al.*, 2003].

[64] To allow zipping, the fore-arc sliver can rotate and/or migrate eastward with the help of a lateral ramp at its NW boundary (Figure 13). The estimated position of the trench zone and the Chortís block relative to North America at 10 Ma implies at most ~10° of counterclockwise rotation. The axis of rotation would be located at the northern tip of the Tonala fault, thus rotation may have produced extension at the NW boundary of the fore-arc sliver (Figure 13). Paleostress tensors younger than 25 Ma [*Meschede et al.*, 1996] derived from striae that were measured at the NW boundary of the fore-arc sliver, agree with the kinematics of the latest structures described along this boundary [*Tolson*, 2007].

[65] We have proposed that the counterclockwise rotation of a fore-arc sliver is due to relative motion of the upper plates above the subduction zone (Figure 11b). In the case of the NACC triple junction, the free boundary is the western end of the Chortís block because it diverges from the subduction zone (Figure 13). This effect could be accelerated by crust weakening. Slab break off in the Cocos plate below the Chortís block [*Rogers et al.*, 2002] produced an ignimbrite flare-up between 17 and 10 Ma from Guatemala to Nicaragua, that may have heated the crust and decreased its strength [*Dupré*, 1970; *Rogers et al.*, 2002; *Jordan et al.*, 2007].

[66] The "zipper" model accounts for the existence of the fore-arc sliver in a region where convergence is not sufficiently oblique to induce strain partitioning [*Jones and Tanner*, 1995; *Teyssier et al.*, 1995]. This model explains why the eastern boundary of the fore-arc sliver, the Tonala fault, was the older prolongation of the sinistral transform boundary (Figure 11b) and why the Tonala fault, north of the PMFS, does not exhibit active strike slip, since it has already sutured. The "zipper" model also explains why the coastal block bordered inland by the Tonala fault appears as the mere northward continuation of the Caribbean fore-arc tectonic sliver and why these blocks are not separated by any prominent fault at the intersection between the projected trace of the PMFS and the subduction zone. Finally, the model allows for the lack of considerable amounts of shortening and extension on the two sides of the transform boundary, as predicted by *Phipps Morgan et al.* [2008].

5.4. Compilation of Existing and New Models of NACC Triple Junction Migration

[67] The "zipper" combined with the "pull-up" models can explain to a large extent the Neogene migration of the NACC triple plate junction. Other processes have been proposed and can be integrated to complement understanding of this triple junction dynamics (Figure 3). Grabens in the extended Chortís block may allow the sliver zone to be easily decoupled from the subduction zone [*Plafker*, 1976; *Gordon and Muehlberger*, 1994; *Rogers et al.*, 2002] (model B, Figure 3). Reverse and strike-slip faults in the North American plate may take up part of the lateral plate motion [*Guzmán-Speziale and Meneses-Rocha*, 2000]. In all models it is recognized that the transform plate motion is distributed over a wide domain, with extension in the Caribbean plate and compression with strike-slip faulting in the North American plate. The observed tectonic pattern can also be explained in part by divergence in strike between the

arcuate, convex to the south sinistral transform boundary and the plate motion vector (model E, Figure 3) [*Burkart and Self*, 1985; *DeMets et al.*, 2000; *Rogers and Mann*, 2007; *Álvarez-Gómez et al.*, 2008; *Rodriguez et al.*, 2009]. *Phipps Morgan et al.* [2008] assign a prominent role to the Cocos plate subduction to explain this tectonic pattern. They propose that the presence of a continuous fore-arc sliver with compression affecting one of the overriding plates, and extension the other, explains the absence of torsion of the Cocos slab at the triple junction (model D, Figure 3).

6. Conclusions

[68] Structural and geomorphic analyses of the plate boundary between the Caribbean and North American plates during Cenozoic time, including the evolution of the Polochic-Motagua fault systems, leads to the following results (Figure 12):

[69] 1. During mid-Miocene to late Miocene, transpressive deformation affected a regional erosion surface that has been developed in mid-Miocene time around the PMFS. South of the Motagua fault, eastward migration of the Caribbean plate generates regional extension in the Chortís block. After late Miocene, extension migrates northward and affects the PMFS. This transpressional tectonic regime goes on today to the north of the Polochic fault.

[70] 2. Recently, the NACC triple junction has become highly diffuse and has propagated eastward by intracontinental deformation. Motion along the PMFS is transferred along new transpressional inland structures in the North American plate east to the Tonala fault and along north to NE trending normal faults in the Chortís block as a horsetail strike-slip fault termination.

[71] 3. Currently, escape motion of the Chortís block is enhanced by intrablock extension and motion on block-bounding faults, the sinistral PMFS and the conjugate dextral WNW trending Jalpatagua fault located along the Pacific margin. The domain west of the Jalpatagua fault is in a fore-arc sliver position.

[72] We propose a combination of plate kinematic models, including the "pull-up" process [*Andreani et al.*, 2008] and a new model that involves a "zipper" process to explain the migration of the NACC triple junction (Figure 11). The "zipper" and "pull-up" models allow blocks of the North American margin to be stripped off in the rear of the fore-arc sliver, dragged into the wake of the Caribbean plate, and eventually incorporated into it, while the fore-arc sliver is progressively transferred from the Caribbean realm to the North American plate. Stretching in the Caribbean plate and shortening in the North American plate help maintain a diffuse triple junction and avoid twisting of the subducting slab. With these processes, a simple North American–Caribbean–Cocos triple junction of rigid plates probably never occurred since continental blocks such as the Chortís block have been involved in Caribbean plate motion.

[73] **Acknowledgments.** This work was funded by the Swiss National Fund grant 200021-112175/1 and an Institute of Technology and the Department of Geology and Geophysics at the University of Minnesota, Minneapolis, UMN grant-in-aid 1003-524-5983. We thank the San Carlos University, Cobán, for fieldwork and administrative and logistical assistance. We acknowledge the local authorities who gave permission to acquire data on their land. We thank Kennet Flores for fruitful discussions and Lothar Ratschbacher, Marco Guzmán-Speziale, and the anonymous reviewer for their comments which improved the manuscript.

References

Álvarez-Gómez, J. A., P. T. Meijer, J. J. Martínez-Díaz, and R. Capote (2008), Constraints from finite element modeling on the active tectonics of northern Central America and the Middle America Trench, *Tectonics*, *27*, TC1008, doi:10.1029/2007TC002162.

Anderson, T. H., and V. A. Schmidt (1983), The evolution of Middle America and the Gulf of Mexico–Caribbean sea region during the Mesozoic, *Geol. Soc. Am. Bull.*, *94*, 941–966, doi:10.1130/0016-7606(1983)94<941:TEOMAA>2.0.CO;2.

Anderson, T. H., B. Burkart, R. E. Clemons, O. H. Bohnenberger, and D. N. Blount (1973), Geology of the western Altos Cuchumatanes, northwestern Guatemala, *Geol. Soc. Am. Bull.*, *84*, 805–826, doi:10.1130/0016-7606(1973)84<805:GOTWAC>2.0.CO;2.

Anderson, T. H., R. J. Erdlac Jr., and M. A. Sandstrom (1985), Late-Cretaceous allochthons and post-Cretaceous strike-slip displacement along the Cuilco-Chixoy-Polochic fault, Guatemala, *Tectonics*, *4*, 453–475, doi:10.1029/TC004i005p00453.

Andreani, L., X. Le Pichon, C. Rangin, and J. Martínez-Reyes (2008), The southern Mexico block: Main boundaries and new estimation for its Quaternary motion, *Bull. Soc. Geol. Fr.*, *179*, 209–223, doi:10.2113/gssgfbull.179.2.209.

Beccaluva, L., S. Bellia, M. Coltorti, G. Dengo, G. Giunta, J. Mendez, J. Romero, S. Rotolo, and F. Siena (1995), The northwestern border of the Caribbean plate in Guatemala: New geological and petrological data on the Motagua ophiolitic belt, *Ofioliti*, *20*, 1–15.

Bellier, O., and M. Zoback (1995), Recent state of stress change in the Walker Lane zone western basin and Range province-USA, *Tectonics*, *14*, 564–593, doi:10.1029/94TC00596.

Brocard, G., C. Teyssier, W. J. Dunlap, C. Authemayou, T. Simon-Labric, L. Chiquín, A. Guttierrez, and S. Morán (2011), Influence of vertical and horizontal displacements on drainage rearrangements along a strike-slip fault, *Basin Res.*, doi:10.1111/j.1365-2117.20011.00510x, in press.

Brueckner, H. K., H. G. Avé Lallemant, V. B. Sisson, G. E. Harlow, S. R. Hemming, U. Martens, T. Tsujimori, and S. S. Sorensen (2009), Metamorphic reworking of a high pressure-low temperature mélange along Motagua fault, Guatemala: A record of Neocomian and Maastrichtian transpressional tectonics, *Earth Planet. Sci. Lett.*, *284*, 228–235, doi:10.1016/j.epsl.2009.04.032.

Burkart, B. (1978), Offset across the Polochic fault of Guatemala and Chiapas, Mexico, *Geology*, *6*, 328–332, doi:10.1130/0091-7613(1978)6<328:OATPFO>2.0.CO;2.

Burkart, B. (1983), Neogene North America–Caribbean plate boundary across northern Central America: Offset along the Polochic fault, *Tectonophysics*, *99*, 251–270, doi:10.1016/0040-1951(83)90107-5.

Burkart, B. (1994), Northern Central America, in *An Introduction: Jamaica, Caribbean Geology*, edited by S. Donavan and T. Jackson, pp. 265–284, UWI Publ. Assoc., Kingston, Jamaica.

Burkart, B., and S. Self (1985), Extension and rotation of crustal blocks in northern Central America and effect on the volcanic arc, *Geology*, *13*, 22–26, doi:10.1130/0091-7613(1985)13<22:EAROCB>2.0.CO;2.

Burkart, B., B. C. Deaton, and G. Moreno (1987), Tectonic wedges and offset Lamaride structures along the Polochic fault of Guatemala and Chiapas, Mexico: Reaffirmation of large Neogene displacement, *Tectonics*, *6*, 411–422, doi:10.1029/TC006i004p00411.

Cáceres, D., D. Monterroso, and B. Tavakoli (2005), Crustal deformation in northern Central America, *Tectonophysics*, *404*, 119–131, doi:10.1016/j.tecto.2005.05.008.

Carey, E. (1979), Recherche des directions principales de contraintes associées au jeu d'une population de failles, *Rev. Geol. Dyn. Geogr. Phys.*, *21*, 57–66.

Carfantan, J. C. (1976), El prolongamiento del sistema de fallas Polochic-Motagua en el sureste de México; una frontera entre dos provincias geologicas, paper presented at III Congresso Latino Americano de Geologia, Acapulco, Mexico.

Carfantan, J. C. (1986), Du système cordillerain nord-américain au domaine caraïbe: Étude géologique du Mexique méridional, Ph.D. thesis, Dep. of Geol., Univ. de Savoie, Chambery, France.

Corredor, F. (2003), Seismic strain rates and distributed continental deformation in the northern Andes and three-dimensional seismotectonics of northwestern South America, *Tectonophysics*, *372*, 147–166, doi:10.1016/S0040-1951(03)00276-2.

DeMets, C. (2001), A new estimate for present-day Cocos-Caribbean plate motion: Implications for slip along the Central American volcanic arc, *Geophys. Res. Lett.*, *28*, 4043–4046, doi:10.1029/2001GL013518.

DeMets, C., P. Jansma, G. S. Mattioli, T. H. Dixon, F. Farina, R. Bilham, E. Calais, and P. Mann (2000), GPS constraints on Caribbean–North America plate motion, *Geophys. Res. Lett.*, *27*, 437–440, doi:10.1029/1999GL005436.

Dengo, C. A. (1982), Structural analysis of the Polochic fault zone in western Guatemala, Central America, Ph.D. thesis, 270 pp., Tex. A&M Univ., College Station.

Dengo, G., O. Bohnenberger, and S. Bonis (1970), Tectonics and volcanism along the Pacific Marginal Zone of Central America, *Geol. Rundsch.*, *59*, 1215–3262.

Dominguez, S., S. E. Lallemand, J. Malavieille, and R. Von Huene (1998), Upper plate deformation associated with seamount subduction, *Tectonophysics*, *293*, 207–224, doi:10.1016/S0040-1951(98)00086-9.

Donnelly, T. W., E. Bocs, S. Reeves, B. Burkart, D. Lawrence, D. Schwartz, W. Newcomb, W. Montgomery, P. Roper, and S. Prucha (1975), Geological map of Guatemala, sheet of the central Motagua River, Inst. Geogr. Nac., Guatemala City, Guatemala.

Donnelly, T. W., G. S. Horne, R. C. Finch, and E. Lopez-Ramos (1990), Northern Central America; the Maya and Chortís blocks, in *The Geology of North America*, vol. H, *The Caribbean Region*, edited by G. Dengo and J. E. Case, pp. 37–76, Geol. Soc. of Am., Boulder, Colo.

Duffield, W. A., G. H. Heiken, K. H. Wohletz, L. W. Maasen, G. Dengo, E. H. Mckee, and O. Castaneda (1992), Geology and geothermal potential of the Tecuamburro volcano area, Guatemala, *Geothermics*, *21*, 425–446, doi:10.1016/0375-6505(92)90001-P.

Dupré, W. R. (1970), Geology of the Zambrano Quadrangle, Honduras, Central America, M. A. thesis, Univ. of Tex. at Austin, Austin.

Fitch, T. J. (1972), Plate convergence, transcurrent faults and internal deformation adjacent to southeast Asia and western Pacific, *J. Geophys. Res.*, *77*, 4432–4460, doi:10.1029/JB077i023p04432.

Flores, K. E. (2009), Mesozoic oceanic terranes of the southern Central America—Geology, geochemistry and geodynamics, Ph.D. thesis, Univ. of Lausanne, Lausanne, Switzerland.

Franco, A., E. Molina, H. Lyon-Caen, J. Vergne, T. Monfret, A. Nercessian, S. Cortez, O. Flores, D. Monterosso, and J. Requenna (2009), Seismicity and crustal structure of the Polochic-Motagua fault system area (Guatemala), *Seismol. Res. Lett.*, *80*, 977–984, doi:10.1785/gssrl.80.6.977.

García-Palomo, A., J. L. Macías, J. L. Arce, J. C. Mora, S. Hughes, R. Saucedo, J. M. Espíndola, R. Escobar, and P. Layer (2006), Geological evolution of the Tacaná Volcanic Complex, México-Guatemala, *Spec. Pap. Geol. Soc. Am.*, *412*, 39–57, doi:10.1130/2006.2412(03).

Gordon, M. B., and H. G. Avé Lallemant (1995), Cryptic strike-slip faults of the Chortís block, *Geol. Soc. Am. Abstr.*, *27*, 227–228.

Gordon, M. B., and W. R. Muehlberger (1994), Rotation of the Chortís block causes dextral slip on the Guayape fault, *Tectonics*, *13*, 858–872, doi:10.1029/94TC00923.

Guzmán-Speziale, M. (2001), Active seismic deformation in the Grabens of northern Central America and its relationships to the relative motion of the northern Central America–Caribbean plate boundary, *Tectonophysics*, *337*, 39–51, doi:10.1016/S0040-1951(01)00110-X.

Guzmán-Speziale, M. (2009), A seismotectonic model for the Chortis block, in *The Origin and Evolution of the Caribbean Plate*, edited by K. H. James et al., *Geol. Soc. Spec. Publ.*, *328*, 197–204, doi:10.1144/SP328.9.

Guzmán-Speziale, M. (2010), Beyond the Motagua and Polochic faults: Active strike-slip faulting along the western North America-Caribbean plate boundary zone, *Tectonophysics*, *496*, 17–27, doi:10.1016/j.tecto.2010.10.002.

Guzmán-Speziale, M., and J. J. Meneses-Rocha (2000), The North America-Caribbean plate boundary west of the Motagua-Polochic fault system: A fault jog in southeastern Mexico, *J. South Am. Sci.*, *13*, 459–468, doi:10.1016/S0895-9811(00)00036-5.

Harlow, G. E., S. R. Hemming, H. G. Avé Lallemant, V. B. Sisson, and S. S. Sorensen (2004), Two high-pressure-low temperature serpentinite-matrix melange belts, Motagua fault zone, Guatemala: A record of Aptian and Maastrichtian collisions, *Geology*, *32*, 17–20, doi:10.1130/G19990.1.

Herrmann, U. R., B. K. Nelson, and L. Ratschbacher (1994), The origin of a terrane: U/Pb zircon geochronology and tectonic evolution of the Xolapa complex, southern Mexico, *Tectonics*, *13*, 455–474, doi:10.1029/93TC02465.

Heuret, A., and S. Lallemand (2005), Plate motions, slab dynamics and back-arc deformation, *Phys. Earth Planet. Inter.*, *149*, 31–51, doi:10.1016/j.pepi.2004.08.022.

Hoke, G. D., and C. N. Garzione (2008), Paleosurfaces, paleoelevation, and the mechanisms for the late Miocene topographic development of the Altiplano plateau, *Earth Planet. Sci. Lett.*, *271*, 192–201, doi:10.1016/j.epsl.2008.04.008.

James, H. K. (2006), Arguments for and against the Pacific origin of the Caribbean Plate: Discussion, finding for an inter-American origin, *Geol. Acta*, *4*, 279–302.

Jones, R. R., and P. W. G. Tanner (1995), Strain partitioning in transpression zones, *J. Struct. Geol.*, *17*, 793–802, doi:10.1016/0191-8141(94)00102-6.

Jordan, B. R., H. Sigurdsson, S. Carey, S. Lundin, R. D. Rogers, B. Singer, and M. Barquero-Molina (2007), Petrogenesis of Central American Tertiary ignimbrites and associated Caribbean Sea tephra, in *Geologic and Tectonic Development of the Caribbean Plate Boundary in Northern Central America*, edited by P. Mann, *Spec. Pap. Geol. Soc. Am.*, *428*, 151–178, doi:10.1130:2007.2428(07).

Keppie, J. D., and J. D. Morán-Zenteno (2005), Tectonic implications of alternative Cenozoic reconstructions for southern Mexico and the Chortís block, *Int. Geol. Rev.*, *47*, 473–491, doi:10.2747/0020-6814.47.5.473.

Kesler, S. E. (1970), Nature of ancestral orogenic zone in nuclear Central America, *AAPG Bull.*, *55*, 2116–2129.

Kesler, S. E., W. L. Josey, and E. M. Collins (1970), Basement rocks of western nuclear Central America: The western Chuacús Group, Guatemala, *Geol. Soc. Am. Bull.*, *81*, 3307–3322, doi:10.1130/0016-7606(1970)81[3307:BROWNC]2.0.CO;2.

La Femina, P. C., T. H. Dixon, and W. Strauch (2002), Bookshelf faulting in Nicaragua, *Geology*, *30*, 751–754, doi:10.1130/0091-7613(2002)030<0751:BFIN>2.0.CO;2.

Leloup, P. H., N. Arnaud, R. Laccassin, J. R. Kienast, T. M. Harrison, T. T. Phan Trong, A. Replumaz, and P. Tapponier (2001), New constraints on the structure, thermochronology, and timing of the Ailao Shan–Red River shear zone, SE Asia, *J. Geophys. Res.*, *106*, 6683–6732, doi:10.1029/2000JB900322.

Lyon-Caen, H., et al. (2006), Kinematics of the North American-Caribbean-Cocos plates in Central America from new GPS measurements across the Polochic-Motagua fault system, *Geophys. Res. Lett.*, *33*, L19309, doi:10.1029/2006GL027694.

McBirney, A. R. (1963), Geology of a part of the Central Guatemalan Cordillera, *Univ. Calif. Publ. Geol. Sci.*, *38*, 177–242.

McCaffrey, R. (1992), Oblique plate convergence, slip vectors, and forearc deformation, *J. Geophys. Res.*, *97*, 8905–8915, doi:10.1029/92JB00483.

McKenzie, D. P., and W. J. Morgan (1969), Evolution of triples junctions, *Nature*, *224*, 125–133, doi:10.1038/224125a0.

Meneses-Rocha, J. J. (2001), Tectonic evolution of the Ixtapa Graben, an example of a strike-slip basin of southeastern Mexico: Implications for regional petroleum systems, in *The Western Gulf of Mexico Basin: Tectonics, Sedimentary Basins and Petroleum Systems*, edited by C. Bartolini, R. T. Buffler, and A. Cantú-Chapa, *AAPG Mem.*, *75*, 183–216.

Mercier, J.-L., E. Carey-Gailhardis, and M. Sébrier (1991), Paleostress determinations from fault kinematics: Application to the Neotectonics of the Himalayas-Tibet and the central Andes, *Philos. Trans. R. Soc. London*, *337*, 41–52, doi:10.1098/rsta.1991.0105.

Meschede, M., W. Frisch, U. R. Herrmann, and L. Ratschbacher (1996), Stress transmission across an active plate boundary: An example from southern Mexico, *Tectonophysics*, *266*, 81–100, doi:10.1016/S0040-1951(96)00184-9.

Minster, J. B., and T. H. Jordan (1978), Present-day plate motions, *J. Geophys. Res.*, *83*, 5331–5354, doi:10.1029/JB083iB11p05331.

Montes, C., Jr., R. D. Hatcher, and P. A. Restrepo-Pace (2005), Tectonic reconstruction of the northern Andean blocks: Oblique convergence and rotations derives from the kinematics of the Piedras-Girardot area, Colombia, *Tectonophysics*, *399*, 221–250, doi:10.1016/j.tecto.2004.12.024.

Mora, J. C., J. L. Macías, A. García-Palomo, J. L. Arce, J. M. Espíndola, P. Manetti, O. Vaselli, and J. M. Sánchez (2004), Petrology and geochemistry of the Tacana volcanic complex, Mexico-Guatemala: Evidence for the last 40000 yr of activity, *Geophys. J. Int.*, *43*, 331–359.

Morgan, W. J., and J. Phipps Morgan (2007), Plate velocities in the hotspot reference frame, in *Plates, Plumes, and Planetary Processes*, edited by G. R. Foulger and D. Jurdy, *Geol. Soc. Am. Spec. Publ.*, *430*, 65–78.

Muehlberger, W. R., and A. W. Ritchie (1975), Caribbean-Americas plate boundary in Guatemala and southern Mexico as seen on Skylab IV orbital photography, *Geology*, *3*, 232–235, doi:10.1130/0091-7613(1975)3<232:CPBIGA>2.0.CO;2.

Newhall, C. G. (1987), Geology of the Lake Atitlan region, western Guatemala, *J. Volcanol. Geotherm. Res.*, *33*, 23–55, doi:10.1016/0377-0273(87)90053-9.

Nieto-Samaniego, A. F., S. A. Alaniz-Álvarez, G. Silva-Romo, M. H. Eguiza-Castro, and C. C. Mendoza-Rosales (2006), Latest Cretaceous to Miocene deformation events in the eastern Sierra Madre del Sur, Mexico, inferred from the geometry and age of major structures, *Geol. Soc. Am. Bull.*, *118*, 238–252, doi:10.1130/B25730.1.

Ortega-Gutiérrez, F., L. Solari, J. Sole, U. Martens, A. Gomez-Tuena, S. Moran-Ical, M. Reyes-Salas, and C. Ortega-Obregon (2004), Polyphase, high temperature eclogite-facies metamorphism in the Chuacus Complex, central Guatemala: Petrology, geochronology, and tectonic implications, *Int. Geol. Rev.*, *46*, 445–470, doi:10.2747/0020-6814.46.5.445.

Ortega-Gutiérrez, F., U. Martens, S. Morán-Icál, M. Chiquín, J. D. Keppie, R. Torres de León, and P. Schaaf (2007), The Maya-Chrotis Boundary: A tectonostratigraphic approach, *Int. Geol. Rev.*, *49*, 996–1024, doi:10.2747/0020-6814.49.11.996.

Phipps Morgan, J. P., C. R. Ranero, and P. Vannucchi (2008), Intra-arc extension in Central America: Links between plate motions, tectonics, volcanism, and geochemistry, *Earth Planet. Sci. Lett.*, *272*, 365–371, doi:10.1016/j.epsl.2008.05.004.

Pindell, J. C., S. C. Cande, W. C. Pitman, D. B. Rowley, J. F. Dewey, J. Labrecque, and W. Haxby (1988), A plate kinematic framework for models of the Caribbean evolution, *Tectonophysics*, *155*, 121–138, doi:10.1016/0040-1951(88)90262-4.

Pindell, J., L. Kennan, W. V. Maresch, K.-P. Stanek, G. Draper, and R. Higgs (2005), Plate-kinematics and crustal dynamics of circum-Caribbean arc-continent interactions, in *Tectonic Controls on Basin Development in Proto-Caribbean Margins*, edited by H. G. Avé-Lallemant and V. B. Sisson, *Spec. Pap. Geol. Soc. Am.*, *394*, 7–52.

Plafker, G. (1976), Tectonic aspects of the Guatemala earthquake of 4 February 1976, *Science*, *193*, 1201–1208, doi:10.1126/science.193.4259.1201.

Ratschbacher, L., et al. (2009), The North American–Caribbean plate boundary in Mexico-Guatemala-Honduras, in *Ice-Marginal and Periglacial Processes and Sediments*, edited by I. P. Martini, H. M. French, and A. Pérez Alberti, *Geol. Soc. Spec. Publ.*, *328*, 219–293, doi:10.1144/SP328.11.

Reynolds, J. H. (1987), Timing and sources of Neogene and Quaternary volcanism in south-central Guatemala, *J. Volcanol. Geotherm. Res.*, *33*, 9–22, doi:10.1016/0377-0273(87)90052-7.

Riller, U., L. Ratschbacher, and W. Frisch (1992), Left-lateral transtension along the Tierra Colorada deformation zone, northern margin of Xolapa magmatic arc of southern Mexico, *J. South Am. Earth Sci.*, *5*, 237–249, doi:10.1016/0895-9811(92)90023-R.

Rodriguez, M., C. DeMets, R. Rogers, C. Tenorio, and D. Hernandez (2009), A GPS and modelling study of deformation in northern Central America, *Geophys. J. Int.*, *178*, 1733–1754, doi:10.1111/j.1365-246X.2009.04251.x.

Rogers, R. D., and P. Mann (2007), Transtensional deformation of the western Caribbean–North America plate boundary zone, *Spec. Pap. Geol. Soc. Am.*, *428*, 37–64, doi:10.1130/2007.2428(03).

Rogers, R. D., H. Kàrason, and R. D. Van der Hilst (2002), Epeirogenic uplift above a detached slab in northern Central America, *Geology*, *30*, 1031–1034, doi:10.1130/0091-7613(2002)030<1031:EUAADS>2.0.CO;2.

Rose, W. I., C. G. Newhall, T. J. Bornhorst, and S. Self (1987), Quaternary silisic pyroclastic deposits of Atitlán caldera, Guatemala, *J. Volcanol. Geotherm. Res.*, *33*, 57–80, doi:10.1016/0377-0273(87)90054-0.

Rosencrantz, E., M. I. Ross, and J. G. Sclater (1988), The age and spreading history of the Cayman trough as determined from depth, heat flow, and magnetic anomalies, *J. Geophys. Res.*, *93*, 2141–2157, doi:10.1029/JB093iB03p02141.

Sallarès, V., and P. Charvis (2003), Crustal thickness constraints on the geodynamic evolution of the Galapagos Volcanic Province, *Earth Planet. Sci. Lett.*, *214*, 545–559, doi:10.1016/S0012-821X(03)00373-X.

Schaaf, P., D. Morán-Zenteno, M. Hernández-Bernal, G. Solís-Pichardo, G. Tolson, and H. Köhler (1995), Paleogene continental margin truncation in southwestern Mexico: Geochronological evidence, *Tectonics*, *14*, 1339–1350, doi:10.1029/95TC01928.

Şengör, A. M. C., B. A. Natal'in, and V. S. Burtlan (1993), Evolution of the Altaid tectonic collage and Palaeozoic crustal growth in Eurasia, *Nature*, *364*, 299–307, doi:10.1038/364299a0.

Shelley, D., and G. Bossière (2002), Megadisplacements and the Hercynian orogen of Gondwanan France and Iberia, *Spec. Pap. Geol. Soc. Am.*, *364*, 209–222.

Sigurdsson, H., S. Kelley, R. M. Leckie, S. Carey, T. Bralower, and J. King (2000), History of circum-Caribbean explosive volcanism: $^{40}Ar/^{39}Ar$ dating of tephra layers, *Proc. Ocean Drill. Program, Sci. Results*, *165*, 299–314, doi:10.2973/odp.proc.sr.165.021.2000.

Silva-Romo, G. (2008), Guayape-Papalutla fault system: A continuous Cretaceous structure from southern Mexico to the Chortís block? Tectonic implications, *Geology*, *36*, 75–78, doi:10.1130/G24032A.1.

Solari, L. A., R. Torres de León, G. Hernández Pineda, J. Solé, G. Solís-Pichardo, and G. Hernández-Treviño (2007), Tectonic significance of Cretaceous–Tertiary magmatic and structural evolution of the northern margin of the Xolapa Complex, Tierra Colorada area, southern Mexico, *Geol. Soc. Am. Bull.*, *119*, 1265–1279, doi:10.1130/B26023.1.

Storti, F., R. E. Holosworth, and F. Salvini (2003), Intraplate strike-slip deformation belts, in *Intraplate Strike-slip Deformation Belts*, edited by F. Storti et al., *Geol. Soc. Spec. Publ.*, *210*, 1–14, doi:10.1144/GSL.SP.2003.210.01.01.

Suski, B., G. Brocard, C. Authemayou, B. C. Muralles, C. Teyssier, and K. Hollinger (2010), Localization and characterization of an active fault in a urbanized area in Central Guatemala by means of geoelectrical imaging, *Tectonophysics*, *480*, 88–98, doi:10.1016/j.tecto.2009.09.028.

Taboada, A., L. A. Rivera, A. Fuenzalida, A. Cisternas, H. Philip, H. Bijwaard, J. Olaya, and C. Rivera (2000), Geodynamics of the northern Andes: Subductions and intracontinental deformation (Colombia), *Tectonics*, *19*, 787–813, doi:10.1029/2000TC900004.

Teyssier, C., B. Tikoff, and M. Markley (1995), Oblique plate motion and continental tectonics, *Geology*, *23*, 447–450, doi:10.1130/0091-7613(1995)023<0447:OPMACT>2.3.CO;2.

Tikoff, B., and C. Teyssier (1994), Strain modeling of displacement-field partitioning in transpressional orogens, *J. Struct. Geol.*, *16*, 1575–1588, doi:10.1016/0191-8141(94)90034-5.

Tolson, G. (2007), The Chacalapa fault, southern Oaxaca, Mexico, *Spec. Pap. Geol. Soc. Am.*, *422*, 343–357, doi:10.1130/2007.2422(12).

Turcotte, D. L., and G. Schubert (Eds.) (2002), *Geodynamics*, 472 pp., Cambridge Univ. Press, Cambridge, U. K.

Van Wyk de Vries, B., P. Grosse, and G. E. Alvarado (2007), Volcanism and volcanic landforms, in *Central America: Geology, Resources, and Hazards*, edited by J. Buschuh and G. E. Alvarado, pp. 1015–1098, Taylor and Francis, London, doi:10.1201/9780203947043.ch4.

Walper, J. L. (1960), Geology of Cobán-Purulha area, Alta Verapaz, Guatemala, *AAPG Bull.*, *44*, 1273–1315.

Wawrzyniec, T., R. S. Molina-Garza, J. Geissman, and A. Iriondo (2005), A newly discovered, relic, transcurrent plate boundary: The Tonala shear zone and paleomagnetic evaluation of the western Maya block, SW Mexico, *Geol. Soc. Am. Abstr. Programs*, *37*, 68.

Weber, B., K. L. Cameron, M. Osorio, and P. Schaaf (2005), A Late Permian tectonothermal event in Grenville crust of the southern Maya Terrane: U-Pb zircon ages from the Chiapas Massif, southeastern Mexico, *Int. Geol. Rev.*, *47*, 509–529, doi:10.2747/0020-6814.47.5.509.

White, R. A., and D. H. Harlow (1993), Destructive upper-crustal earthquakes of Central America since 1900, *Bull. Seismol. Soc. Am.*, *83*, 1115–1142.

Widdowson, M. (1997), The geomorphological and geological importance of paleosurfaces, in *Paleosurfaces: Recognition, Reconstruction and Paleoenvironmental Interpretation*, edited by M. Widdowson, *Geol. Soc. Spec. Publ.*, *120*, 1–12, doi:10.1144/GSL.SP.1997.120.01.01.

Williams, H., and A. R. McBirney (1969), Volcanic history of Honduras, *Univ. Calif. Publ. Geol. Sci.*, *85*, 1–70.

Wunderman, R. L., and W. I. Rose (1984), Amatitlan, an active resurging cauldron 10 km south of Guatemala city, *J. Geophys. Res.*, *89*, 8525–8539, doi:10.1029/JB089iB10p08525.

C. Authemayou, Laboratoire Domaines Océaniques, UMR 6538, Université Européenne de Bretagne, IUEM, Place Copernic, F-29280 Plouzané, France. (christine.authemayou@univ-brest.fr)

G. Brocard, Department of Earth and Environmental Sciences, University of Pennsylvania, 240 South 33rd St., Philadelphia, PA 19104-6316, USA. (gbrocard@sas.upenn.edu)

N. E. Chiquín, A. Guttiérrez, and S. Morán, Department of Geology, Universitad de San Carlos, Centro Universitario del Noreste, Coban, Guatemala. (noeggeon@gmail.com; ing_geo_axelgutierrez@hotmail.com; sergiomical@yahoo.com)

T. Simon-Labric, ISterre, Université de Grenoble, BP 53, F-38041 Grenoble CEDEX, France. (thibaud.simon-labric@ujf-grenoble.fr)

C. Teyssier, Department of Geology and Geophysics, University of Minnesota–Twin Cities, Minneapolis, MN 55455, USA. (teyssier@umn.edu)